References

1. FUJII, T. and T. ARAKI, *A kinetic study on descarburization in molten steel.* Tetsu-to-Hogané Overseas, 1965. **5**(No. 4): p. 290-302.
2. GHOSH, D.N., *Kinetics of the decarburization of Fe-C melts: Part 1 high carbon levels.* Ironmaking and Steelmaking (Quaterly), 1975. **1**: p. 36-44.
3. GHOSH, D.N., *Kinetics of the decarburization of Fe-C melts: Part 2 low carbon levels.* Ironmaking and Steelmaking (Quaterly), 1975. **1**: p. 45-48.
4. NOMURA, H. and K. MORI, *Kinetics of decarburization of liquid-Iron with high-concentration of carbon.* Transactions of ISIJ, 1973. **13**(4): p. 265-273.
5. NOMURA, H. and K. MORI, *Kinetics of decarburization of liquid-iron at low concentrations of carbon.* Transactions of ISIJ, 1973. **13**(1): p. 325-333.
6. SZEKELY, J. and M.R. TODD, *A Note on Reaction Mechanism of Carbon Oxidation in Oxygen Steelmaking Processes.* Transactions of the Metallurgical Society of Aime, 1967. **239**(10): p. 1664-1666.
7. SIDENOR, G., *Technical Report Oxygen Solubility in Steel*. 2005, Gerdau Sidenor.
8. TURKDOGAN, E., *Fundamentals of Steelmaking*. 1996: The Institute of Materials.
9. Fruehan, R.J., *Fundamentals of Iron and Steelmaking*, in *The making, shaping, and treating of steel*, R.J. Fruehan, Editor. 1998, AISE Steel Foundation. p. 13-152.
10. TURKDOGAN, E. *Equilibrium and Non-Equilibrium States in Steelmaking* in *Turkdogan Symposium Proceedings*. 1994.
11. OETERS, F., *(7) Reactor Theory*, in *Metallurgy of Steelmaking*. 1994, Verlag Stahleisen mbH.
12. SUN, H.P. and R.D. PEHLKE, *Modeling and experimental study of gaseous oxidation of liquid iron alloys.* Metallurgical and Materials Transactions B-Process Metallurgy and Materials Processing Science, 1996. **27**(5): p. 854-864.
13. WIDLUND, D., D.S. SARMA, and P.G. JONSSON, *Studies on decarburisation and desiliconisation of levitated Fe-C-Si alloy droplets.* ISIJ International, 2006. **46**(8): p. 1149-1157.
14. DEO, B.B.V. *Application of Model Predictive Control in Dynamic System: An Application to BOF Steelmaking Process*. in *AISTech 2009 Proceedings* 2009.
15. CAMPOS, V.F., *Tecnologia de Fabricação do Aço Líquido*. 3.a ed. 1985: Universidade Federal de Minas Gerais - UFMG.
16. GOTO, K., M. KAWAKAMI, and M. SOMENO, *On rate of decarburization of liquid metals with CO-CO_2 gas mixture.* Transactions of the Metallurgical Society of Aime, 1969. **245**(2): p. 293-301.

17. BAKER, L.A., N.A. WARNER, and A.E. JENKINS, *Kinetics of decarburization of liquid iron in oxidizing atmosphere using levitation technique.* Transactions of the Metallurgical Society of Aime, 1964. **230**(6): p. 1228-1235.
18. LEE, H.G. and Y.K. RAO, *Decarburization and nitrogen absorption in molten Fe-C alloys: Part 2 Mathematical-model.* Ironmaking & Steelmaking, 1988. **15**(5): p. 238-243.
19. SIMENTO, N., H.G. LEE, and P.C. HAYES, *Kinetics of decarburisation of levitating iron drops by oxygen.* Steel Research, 1998. **69**(9): p. 349-354.
20. BAKER, L.A., N.A. WARNER, and A.E. JENKINS, *Decarburization of a levitated iron droplet in oxygen.* Transactions of the Metallurgical Society of Aime, 1967. **239**(6): p. 857-864.
21. GHOSH, D.N. and P.K. SEN, *Kinetics of decarburization of iron-carbon melts in oxidizing gas atmospheres.* Journal of the Iron and Steel Institute, 1970. **208**: p. 911-916.
22. GUNJI, K., *Kinetics of decarburization of liquid iron in an oxidizing atmosphere.* Transactions of the Iron and Steel Institute of Japan, 1970. **10**(1): p. 1-12.
23. FRUEHAN, R.J. and L.J. MARTONIK, *Rate of decarburization of liquid-iron by CO_2 and H2.* Metallurgical Transactions, 1974. **5**(5): p. 1027-1032.
24. SAIN, D.R. and G.R. BELTON, *Interfacial reaction-kinetics in decarburization of liquid-iron by carbon-dioxide.* Metallurgical Transactions B-Process Metallurgy, 1976. **7**(2): p. 235-244.
25. SWISHER, J.H. and E.T. TURKDOGAN, *Decarburization of iron-carbon melts in CO_2-CO atmospheres - kinetics of gas-metal surface reactions.* Transactions of the Metallurgical Society of Aime, 1967. **239**(5): p. 602-610.
26. FRUEHAN, R.J. and F.J. MANNION, *Decarburization kinetics of liquid Fe-Csat alloys by CO_2.* Metallurgical Transactions B-Process Metallurgy, 1989. **20**(6): p. 853-861.
27. BELTON, G.R., *Langmuir adsorption, Gibbs adsorption-isotherm, and interfacial kinetics in liquid-metal systems.* Metallurgical Transactions B-Process Metallurgy, 1976. **7**(1): p. 35-42.
28. KAWAI, Y. and K. MORI, *Equilibrium and kinetics of slag-metal reactions.* Transactions of the Iron and Steel Institute of Japan, 1973. **13**(5): p. 303-317.
29. LI, K., D.A. DUKELOW, and G.C. SMITH, *Decarburization in iron-carbon system by oxygen top blowing.* Transactions of the Metallurgical Society of Aime, 1964. **230**(1): p. 71-76.
30. POVOLOTSKI, D.Y. and Y.A. GUDIM, *The Kinetics of Steel Decarburization in Electric-Arc Furnaces.* Russian Metallurgy, 1993(5): p. 17-21.
31. FORTES, R., H. MATSUURA, and R. FRUEHAN. *Decarburization and Slag Formation Model for the Electric Arc Furnace*. in *AISTech*. 2008. Pittsburgh, PA: AIST.

32. IWAMASA, P.K. and R.J. FRUEHAN, *Separation of metal droplets from slag.* ISIJ International, 1996. **36**(11): p. 1319-1327.
33. LI, Y. and I.P. RATCHEV, *Rate of interfacial reaction between molten CaO-SiO_2-Al_2O_3-Fe_xO and CO-CO_2.* Metallurgical and Materials Transactions B-Process Metallurgy and Materials Processing Science, 2002. **33**(5): p. 651-660.
34. MIN, D.J. and R.J. FRUEHAN, *Rate of Reduction of FeO in Slag by Fe-C Drops.* Metallurgical Transactions B-Process Metallurgy, 1992. **23**(1): p. 29-37.
35. SMITH, R.H. and R.J. FRUEHAN, *The effect of carbon content on the rate of reduction of FeO in slag relevant to iron smelting.* Steel Research, 1999. **70**(8-9): p. 283-295.
36. MIN, D.J., J.W. HAN, and W.S. CHUNG, *A study of the reduction rate of FeO in slag by solid carbon.* Metallurgical and Materials Transactions B-Process Metallurgy and Materials Processing Science, 1999. **30**(2): p. 215-221.
37. OZAWA, M., et al., *Reduction of FeO in molten slags by solid carbon in the electric-arc furnace operation.* Transactions of the Iron and Steel Institute of Japan, 1986. **26**(7): p. 621-628.
38. SARMA, B., A.W. CRAMB, and R.J. FRUEHAN, *Reduction of FeO in smelting slags by solid carbon: Experimental results.* Metallurgical and Materials Transactions B-Process Metallurgy and Materials Processing Science, 1996. **27**(5): p. 717-730.
39. STORY, S.R., et al., *Reduction of FeO in smelting slags by solid carbon: Re-examination of the influence of the gas-carbon reaction.* Metallurgical and Materials Transactions B-Process Metallurgy and Materials Processing Science, 1998. **29**(4): p. 929-932.
40. SEO, K. and R.J. FRUEHAN, *Reduction of FeO in slag with coal char.* ISIJ International, 2000. **40**(1): p. 7-15.
41. POIRRIER D.; GEIGER, G., *Transport Phenomena in Materials Processing*. 1994: TMS The Minerals, Metals and Materials Society.
42. GAYE, H., P. DESTANNES, and J. ROTH. *Kinetics of Scrap Dissolution in the Converter and Electric Arc Furnace*. in *The Sixth International Iron and Steel Congress ISIJ*. 1990: ISIJ.
43. GAYE, H., et al., *Kinetics of Scrap Dissolution in the Converter - Theoretical-Model and Plant Experimentation.* Revue De Metallurgie-Cahiers D Informations Techniques, 1986. **83**(11): p. 793-806.
44. GUTHRIE, R.I. and P. STUBBS, *Isothermal Scrap Melting Rates in Pig-Iron Baths.* Canadian Mining and Metallurgical Bulletin, 1972. **65**(724): p. 20-28.
45. GUTHRIE, R.I. and P. STUBBS, *Kinetics of Scrap Melting in Baths of Molten Pig-Iron.* Canadian Metallurgical Quarterly, 1973. **12**(4): p. 465-473.

46. LOMMEL, J.M. and B. CHALMERS, *The Isothermal Transfer from Solid to Liquid in Metal Systems.* Transactions of the American Institute of Mining and Metallurgical Engineers, 1959. **215**(3): p. 499-508.
47. MORI, K. and T. SAKURAYA, *Rate of Dissolution of Solid Iron in a Carbon-Saturated Liquid-Iron Alloy with Evolution of Co.* Transactions of the Iron and Steel Institute of Japan, 1982. **22**(12): p. 984-990.
48. OLSSON, R.G., V. KOUMP, and T.F. PERZAK, *Rate of Dissolution of Carbon-Steel in Molten Iron-Carbon Alloys.* Transactions of the Metallurgical Society of Aime, 1965. **233**(9): p. 1654-1657.
49. PEHLKE, R.D., P.D. GOODELL, and R.W. DUNLAP, *Kinetics of Steel Dissolution in Molten Pig Iron.* Transactions of the Metallurgical Society of Aime, 1965. **233**(7): p. 1420-1427.
50. SZEKELY, J., Y.K. CHUANG, and J.W. HLINKA, *Melting and Dissolution of Low-Carbon Steels in Iron-Carbon Melts.* Metallurgical Transactions, 1972. **3**(11): p. 2825-2833.
51. WRIGHT, J.K., *Steel Dissolution in Quiescent and Gas Stirred Fe/C Melts.* Metallurgical Transactions B-Process Metallurgy, 1989. **20**(3): p. 363-374.
52. DENHARTOG, H.W., P.J. KREYGER, and A.B. SNOEIJER, *Dynamic Model of Dissolution of Scrap in the BOF Process.* C.R.M., 1973. **37**: p. 13-22.
53. LI, J.H. and N. PROVATAS, *Kinetics of scrap melting in liquid steel: Multipiece scrap melting.* Metallurgical and Materials Transactions B-Process Metallurgy and Materials Processing Science, 2008. **39**(2): p. 268-279.
54. Fortes, R., *Gerdau private communication*. 2006.
55. HU, H. and S.A. ARGYROPOULOS, *Mathematical modelling of solidification and melting: A review.* Modeling and Simulation in Materials Science and Engineering, 1996. **4**(4): p. 371-396.
56. Friedric.Ha, O. Knacke, and H. Jauer, *Limiting Cases of Dissolution of a Solid in Its Own Melt.* Archiv Fur Das Eisenhuttenwesen, 1973. **44**(12): p. 879-886.
57. FRIEDRICHS, H.A., O. KNACKE, and H. JAUER, *Limiting Cases of Dissolution of a Solid in Its Own Melt.* Archiv Fur Das Eisenhuttenwesen, 1973. **44**(12): p. 879-886.
58. OETERS, F., *(8) The Kinetics of Melting*, in *Metallurgy of Steelmaking*. 1994, Verlag Stahleisen mbH.
59. EHRICH, O., Y.K. CHUANG, and K. SCHWERDTFEGER, *Melting of Metal Spheres Involving Initially Frozen Shells with Different Material Properties.* International Journal of Heat and Mass Transfer, 1978. **21**(3): p. 341-349.
60. EHRICH, O., Y.K. CHUANG, and K. SCHWERDTFEGER, *Melting of Sponge Iron Spheres in Their Own Melt.* Archiv Fur Das Eisenhuttenwesen, 1979. **50**(8): p. 329-334.

61. GOURTSOY.L and R. GUTHRIE, *Melting Rates of Furnace and Ladle Additions in Steelmaking Processes.* Canadian Mining and Metallurgical Bulletin, 1971. **64**(712): p. 37-46.
62. Provatas, N., G. Brooks, and J.H. Li, *Steel Scrap Melting in Liquid Steel*. 2004, McMaster university, SCR Meeting: Hamilton, CA.
63. PROVATAS, N. and J.H. LI, *Kinetics of Steel Scrap Melting*. 2006, McMaster University, SCR Meeting: Hamilton.
64. Trotter, D.C., G.;Rafiei, P.; Honeyands, T., *Understanding the Melting Characteristics of HBI in iron and Steel Melts.* SEAISI Quarterly, 2005. **34**(1): p. 16-28.
65. LI, J.H., G. BROOKS, and N. PROVATAS, *Kinetics of scrap melting in liquid steel.* Metallurgical and Materials Transactions B-Process Metallurgy and Materials Processing Science, 2005. **36**(2): p. 293-302.
66. SPECHT, E. and R. JESCHAR, *Kinetics of Steel Melting in Carbon-Steel Alloys.* Steel Research, 1993. **64**(1): p. 28-34.
67. ASAI, S., et al., *Mixing time of refining vessels stirred by gas injection.* Transactions of the Iron and Steel Institute of Japan, 1983. **23**(1): p. 43-50.
68. TROTTER, D., P. RAFIEI, and T. HONEYANDS, *Understanding the melting characteristics of HBI in iron and steel melts.* SEASI Quaterly, 2005. **34**(1): p. 16-28.
69. PROVATAS, N., G. BROOKS, and J.H. LI, *Steel Scrap Melting in Liquid Steel*. 2005, McMaster university, SCR Meeting: Hamilton, CA.
70. BAUMERT, J., et al., *Improved control of electric arc furnace operations by process modelling*. 2003, European Commission - Steelmaking Processes.
71. RIZZO, E., *Introdução aos Processos de Refino Primário no Forno Elétrico a Arco*, ed. A.B.d.M.e.M.-. ABM. 2006.
72. MANNING, C., *Behavior of Phosphorus in DRI/HBI During Electric Furnace Steelmaking*, in *Department of Materials Science and Engineering*. 2000, Carnegie Mellon University: Pittsburgh.
73. BEKKER, J.G., I.K. CRAIG, and P.C. PISTORIUS, *Modeling and simulation of an electric arc furnace process.* ISIJ International, 1999. **39**(1): p. 23-32.
74. MORALES, R.D., RODRIGUEZ, H.H., ROMERO, A.S., LULE, R., CAMACHO, J. *Design of Metallurgical Practices for EAF Through Mathematical Modelling*. in *Electric Furnace Conference Proceedings*. 1995.
75. LACHMUND, H.B., NORBERT; . *Comparative Assessment of LD Converter and Electric Arc Furnace Steelmaking in Terms of Removal of Undesirable Tramp Elements*. in *AISTech 2008*. 2008. Pittsburg PA.
76. THOMSON, M.J., et al., *Control of greenhouse gas emissions from electric arc furnace steelmaking: evaluation methodology with case studies.* Ironmaking & Steelmaking, 2000. **27**(4): p. 273-279.

77. MATHUR, P. in *51st Electric Furnace Conference Proc*. 1993. Warrendale, PA.
78. DEO, B. and R. BOOM, *Fundamentals of Steelmaking Metallurgy*. Fundamentals of Steelmaking Metallurgy. 1993: Prentice-Hall International. 194.
79. SANO, K. and K. ITO, *Decarburization of molten iron and oxidation of coexistent elements.* Transactions ISIJ, 1968. **8**: p. 165-171.
80. Goldstein, D., *Nitrogen Removal Phenomena*. 2002, Carnegie Mellon University: Pittsburgh.
81. YAMAGATA, C. and T. MIYAKE, *Desiliconization Reaction of Pig Iron with High FeO Containing Blast Furnace Slag under Pressurized and Coke-coexisting Condition.* ISIJ International, 1990. **30**(9): p. 740-747.
82. IDE, K.F., R.J., *Evaluation of phosphorus reaction equilibrium in steelmaking.* Iron & Steelmaker, 2000. **27**(12): p. 65-70.
83. KITAMURA, S., et al., *Analysis of Dephosphorization Reaction Using a Simulation Model of Hot Metal Dephosphorization by Multiphase Slag.* ISIJ International, 2009. **49**(9): p. 1333-1339.
84. KITAMURA, S.Y., et al., *Development of Analysis and Control Method for Hot Metal Dephosphorization Process by Computer-Simulation.* ISIJ International, 1991. **31**(11): p. 1329-1335.
85. KITAMURA, S.Y., et al., *Effect of Stirring Energy, Temperature and Flux Composition on Hot Metal Dephosphorization Kinetics.* ISIJ International, 1991. **31**(11): p. 1322-1328.
86. WEI, P., et al., *Estimation of Slag Metal Interfacial Oxygen Potential in Phosphorus Reaction between Fe(T)O Containing Slag and Molten Iron of High-Carbon Concentration.* ISIJ International, 1993. **33**(8): p. 847-854.
87. WEI, P., et al., *Kinetics of Phosphorus Transfer between Iron-Oxide Containing Slag and Molten Iron of High-Carbon Concentration under Ar-O_2 Atmosphere.* ISIJ International, 1993. **33**(4): p. 479-487.
88. CHAM, S.T., et al., *Factors influencing carbon dissolution from cokes into liquid iron.* ISIJ International, 2004. **44**(11): p. 1835-1841.
89. MOURAO, M., M. KRISHNA, and J. ELLIOT, *Experimental Investigation of Dissolution Rates of Carbonaceous Materials in Liquid Iron-Carbon Melts.* Metallurgical Transactions B, 1993. **24B**: p. 629-637.
90. RAHMAN, M., et al., *The Influence of Ash Impurities on Interfacial Reactions between Carbonaceous Materials and EAF Slag at 1550 C.* ISIJ International, 2009. **49**(3): p. 329-336.
91. SUN, H.P., *Analysis of reaction rate between solid carbon and molten iron by mathematical models.* ISIJ International, 2005. **45**(10): p. 1482-1488.
92. WRIGHT, J.K. and B.R. BALDOCK, *Dissolution Kinetics of Particulate Graphite Injected into Iron Carbon Melts.* Metallurgical Transactions B-Process Metallurgy, 1988. **19**(3): p. 375-382.

93. LEVENSPIEL, O., *(25) Fluid-Particle Reactions: Kinetics*, in *Chemical Reaction Engineering*. 1999, John Wiley & Sons.

94. WENDELSTORF, J., *Analysis of the EAF operation by process modelling.* Archives of Metallurgy and Materials (Poland), 2008. **53**(2): p. 385-390.

95. ELLIS, A.F. and J. GLOVER, *Mechanism of Fume Formation in Oxygen Steelmaking.* Journal of the Iron and Steel Institute, 1971. **209**(AUG): p. 593-599.

96. POTEY, D. and B. BOWMAN, *Electrode Consumption Model*, in *8th European Electric Steelmaking Conference*. 2005: Birmingham, UK.

97. MATSUURA, H., R. FORTES, and R.J. FRUEHAN, *Development of a decarburization and slag formation model for the electric arc furnace.* ISIJ International, 2008. **48**(9): p. 1197-1205.

98. GUTHRIE, R.I.L., *Engineering In Process Metallurgy*. 1989: Oxford University Press.

99. COSTA E SILVA, A., *Termodinâmica Aplicada a Aciaria*. 1999: Universidade Federal Fluminense.

100. MATHUR, P., *Praxair CoJet ^{tm} Technology • Principles and Actual Results from Recent Installations.* AISE Steel Technology, 2000. **78**(5): p. 21-25.

101. EVENSON, E.J., J. GUERARD, and H.D. GOODFELLOW. *Energy Optimization and Continuous Fume Analysis at Co-Steel LASCO*. in *Proceedings of the 55th Electric Furnace Conference,*. 1997. Chicago.

102. EVENSON, E.J., H.D. GOODFELLOW, and M.J. KEMPE. *EAF Process Optimization through Off-Gas Analysis and Closed-Loop Process Control at Deacero, Saltillo, Mexico*. in *Electric Furnace Conference Proceedings*. 2000.

103. FRUEHAN, R.J., *Rate of Reduction of Iron-Oxides by Carbon.* Metallurgical Transactions B-Process Metallurgy, 1977. **8**(2): p. 279-286.

104. TURKDOGAN, E.T. and J. PEARSON, *Activities of Constituents of Iron and Steelmaking Slags .1. Iron Oxide.* Journal of the Iron and Steel Institute, 1953. **173**(3): p. 217-223.

105. BASU, S., A. LAHIRI, and S. SEETHARAMAN, *Activity of Iron Oxide in Steelmaking Slag.* Metallurgical and Materials Transactions B, 2008. **39B**: p. 447-456.

106. STAHLUNDEISEN, *Slag Atlas*. 2nd Edition ed. 1995: Verein Deutscher Eisenhuttenleute

107. BANYA, S., *Mathematical expression of slag metal reactions in steelmaking process by quadratic formalism based on the regular solution model.* ISIJ International, 1993. **33**(1): p. 2-11.

108. MORALES, A. and R. FRUEHAN, *Thermodynamics of MnO, FeO, and Phosphorus in Steelmaking Slags with High MnO Contents.* Metallurgical and Materials Transactions B, 1997. **28B**: p. 1111-1118.

109. FRUEHAN, R.J., *CISR notes on iron oxide reduction rate*, R. Fortes, Editor. 2009.

110. TEASDALE, S.L. and P.C. HAYES, *Kinetics of reduction of FeO from slag by graphite and coal chars.* ISIJ International, 2005. **45**(5): p. 642-650.

111. PRETORIUS, E. and R. CARLISLE. *Foamy Slag Fundamentals and their Practical Application to Electric Furnace Steelmaking*. in *Electric Furnace Conference Proceedings*. 1998.

112. PINDAMONHANGABA, E., *Soluble oxygen measurements*. 2008, Gerdau

113. BRABIE, L.C. and M. KAWAKAMI, *Kinetics of steel scrap melting in molten Fe-C bath.* High Temperature Materials and Processes, 2000. **19**(3-4): p. 241-255.

114. KAWAKAMI, M., K. TAKATANI, and L.C. BRABIE, *Heat and mass transfer analysis of scrap melting in steel bath.* Tetsu to Hagane-Journal of the Iron and Steel Institute of Japan, 1999. **85**(9): p. 658-665.

115. NASCIMENTO, C.B., B., *Gerdau confidential report*. 2007: Rio de Janeiro.

116. GASKELL, D.R., *Introduction to the thermodynamics of materials*. Fourth Edition ed. 2003, New York: Taylor & Francis. 618 p.

117. VENSEL, D., H. HENEIN, and P.H. DAUBY, *A thermodynamic analysis of decarburization and post combustion in BOP.* I&SM, 1987(February): p. 45-52.

118. UPADHYAYA, G.D., R., *Problems in Metallurgical Thermo-dynamics and Kinetics*. International Series in Materials Science & Technology. Vol. 25. 1977: Pergamon International Library.

119. ADAMIAN, R.A., E., *Físico-Química - Uma Aplicação aos Materiais*. 2002: COPPE - Universidade Federal do Rio de Janeiro UFRJ.

120. INCROPERA F., D.D., BERGMAN T., LAVINE A, *Fundamentos de Transferência de Calor e de Massa* 6th ed. 2008.

Appendices 1 – Short Literature Review on Melting Experimental Apparatus

Publishing	**Author**	**R Olsson**		**D Pehlke**	**R Guthrie**	**R Guthrie**	**D Pehlke**	**K Mori**	**J Wright**	**G Brooks**
	Year	1965		1965	1971	1973	1974	1982	1989	2005
	Institution	US Steel Corp		Univ of Michigan	McGill Univ	McGill Univ	Univ of Michigan	Nagoya Univ	CSIRO	McMaster
		High C Bath Low C Sample	Medium C Bath Low C Sample	High and Medium C Bath Low C Sample	High C Bath Medium C Sample	High and Medium C Bath Low C Sample	High C Bath Low and Medium C Sample	High C Bath Low C Sample (several Oxygen content in the solid samples)	High C Bath Low C Sample	Low Carbon Bath Low Carbon Sample
Conclusions	**Controlling rate mechanism and dissolution rates**	Limited by mutual counterdiffusion of Fe and C in the boundary Layer		LPMT Boundary-layer diffusion (Carbon)	LPMT Boundary-layer diffusion		The solution rate was found to be controlled by LPMT.	LPMT Boundary-layer diffusion (Carbon)	LPMT Boundary-layer diffusion (Carbon)	Heat Transfer is the limiting process
		Melting rate increases with rotation rate		The rate of dissolution of steel in molten pig iron is increased by increased temperature, increased composition gradients and increased stirring	Thermal convection currents were generated by liquid density gradients	Mass Transfer was dominated by natural convection	Mass Transfer was dominated by natural convection when the sample was stationary and by forced convection when rotated	Melting rate increases with rotation and with CO bubles evolution (increases with %O in the solid sample)	Increases with Carbon in the bath	Oxide layer at sample surface does not affect the melting rate
									Increases with stirring flow rate	
		Increases with Temperature								
				Melting rate decreases with sample size						
		Steelberg formations		Steelberg formations	Steelberg formations					Steelberg formations
		Mass Transfer coefficient								
		$m = (const)^{0.7}$			$m = \frac{\frac{\rho_S}{\rho_L} C_L^i - C_S^0}{C_L^0 - C_L^i} \frac{dr}{dt}$		Transport coefficients were fitted to dimensionless correlations for mass transfer	Mass transfer coefficients are calculated	Mass transfer coefficients are calculated	
	Modeling	Isothermal and steady state		Isothermal and steady state	Heat transfer unsteady-state		Isothermal and steady state			Phase-field Model
	Limitations				Unknown physical properties of solid close to the melting point cuased significant model errors	Mass transfer coefficients had to be corrected for the effects of shrinking interface			Apparatus geometry interfers on mass transfer coefficient	Heat conductivity is not constant over the whole solid phase

Publishing	Author		R Olsson		D Pehlke	R Guthrie	R Guthrie	D Pehlke	K Mori		J Wright		G Brooks
	Year		1965		1965	1971	1973	1974	1982		1989		2005
	Institution		US Steel Corp		Univ of Michigan	McGill Univ	McGill Univ	Univ of Michigan	Nagoya Univ		CSIRO		McMaster
			High C Bath Low C Sample	Medium C Bath Low C Sample	High and Medium C Bath Low C Sample	High C Bath Medium C Sample	High and Medium C Bath Low C Sample	High C Bath Low and Medium C Sample	High C Bath Low C Sample (several Oxygen content in the solid samples)		High C Bath Low C Sample		Low Carbon Bath Low Carbon Sample
			$m = (const)^{0.7}$										
Liquid Bath	Chemical Composition	%C	1.5%-4.5%		4,25%	5%	4.7%-2.8%	4,25%	4,25%		2.0%-4.5%	3.7%-4.3%	0.15%-0.20%
		%Si			0,80%		1,1%						
		%Mn			0,50%								0.60%-0.90%
		ppm Soluble O											
		Raw Materials			Electrolitic Fe and purity electrode graphite		Remelted blast furnace iron-C	Electrolitic Fe and purity electrode graphite			Electrolitic Fe and purity electrode graphite		
	Temperature	°C	1250 up to 1500		1260-1370-1455	1320-1400	1260-1455	(5 Levels) 1185-1406	(6 Levels) 1200-1450		1260-1460	1400	1650
		Accuracy °C						+/- 7					+/- 5
								Isothermal	Isothermal		Isothermal		Isothermal
	Top Shrounding	Gas					Coke	Argon	Argon		N_2	N_2	Ar 99.99%
		Flow Rate (SL/min)							0,7		2		1,0
	Controlled Atmosphere							Argon					
	Stirring	Gas									N_2	N_2	
		Flow Rate									up to 6	5-40	
	Sample Mode	mode	Rotary		Stationary	Rotary and Induction	Stationary	Stationary	Rotary	Stationary (with and without CO evolution)	Rotary (with and without CO evolution)	Stationary and Gas Stirring	Stationary
		rpm	(15 levels) 32 - 1210			200			(5 levels) 450 - 1800		(4 levels) 95 - 900		
	Bath Sampling	Chemistry			Intermitent sampling		Yes						
		Temperature					Yes						
	Convection		Forced by rotation samples		Natural Convection	Stirring by induction magnetic field and rotation					Turbulent Natural (Forced effects minimized by switching off power)		Natural (Forced effects minimized by switching off power)
	Experiment time	sec	25-120		30-360	3-30		60-840			5-30	5-100	5-80

Publishing	**Author**		**R Olsson**	**D Pehlke**		**R Guthrie**	**R Guthrie**	**D Pehlke**	**K Mori**		**J Wright**		**G Brooks**
	Year		1965	1965		1971	1973	1974	1982		1989		2005
	Institution		US Steel Corp	Univ of Michigan		McGill Univ	McGill Univ	Univ of Michigan	Nagoya Univ		CSIRO		McMaster
Liquid Bath	Chemical Composition	%C	1.5%-4.5%	4,25%		5%	4.7%-2.8%	4,25%	4,25%		2.0%-4.5%	3.7%-4.3%	0.15%-0.20%
		%Si		0,80%			1,1%						
		%Mn		0,50%									0.60%-0.90%
		ppm Soluble O											
		Raw Materials		Electrolitic Fe and purity electrode graphite			Remelted blast furnace iron-C	Electrolitic Fe and purity electrode graphite			Electrolitic Fe and purity electrode graphite		
	Temperature	°C	1250 up to 1500	1260-1370-1455		1320-1400	1260-1455	(5 Levels) 1185-1406	(6 Levels) 1200-1450		1260-1460	1400	1650
		Accuracy °C						+/- 7					+/- 5
								Isothermal	Isothermal		Isothermal		Isothermal
	Top Shrounding	Gas					Coke	Argon	Argon		N_2	N_2	Ar 99.99%
		Flow Rate (SL/min)							0,7		2		1,0
	Controlled Atmosphere							Argon					
	Stirring	Gas									N_2	N_2	
		Flow Rate									up to 6	5-40	
	Sample Mode	mode	Rotary	Stationary	Rotary and Induction	Stationary		Stationary	Rotary	Stationary (with and without CO evolution)	Rotary (with and without CO evolution)	Stationary and Gas Stirring	Stationary
		rpm	(15 levels) 32 - 1210		200				(5 levels) 450 - 1800		(4 levels) 95 - 900		
	Bath Sampling	Chemistry		Intermitent sampling			Yes						
		Temperature					Yes						
	Convection		Forced by rotation samples	Natural Convection	Stirring by induction magnetic field and rotation							Turbulent Natural (Forced effects minimized by switching off power)	Natural (Forced effects minimized by switching off power)
	Experiment time	sec	25-120	30-360		3-30		60-840				5-30	5-100	5-80

Publishing	**Author**		**R Olsson**		**D Pehlke**	**R Guthrie**	**R Guthrie**	**D Pehlke**		**K Mori**	**J Wright**		**G Brooks**
	Year		1965		1965	1971	1973	1974		1982	1989		2005
	Institution		US Steel Corp		Univ of Michigan	McGill Univ	McGill Univ	Univ of Michigan		Nagoya Univ	CSIRO		McMaster
Solid Sample	Chemical Composition	%C	0,008	1,00	0,20	0,85%		0,007%	0,44%	0.002%-0.005%	0,26%		0.15%-0.20%
		%Si	0	0		0,40%		0	0	0.001%-0.005%			
		%Mn	0	0		0,30%		0	0	0.001%-0.003%	0,70%		0.60%-0.90%
		%S								0.002%-0.005%			
		ppm O								(11 levels) 0-11400			
		Raw Material			1020 Commercial		Low C commercial				Commercial		
	Oxidation layer				Cleaned samples								Yes
	Pre-heating	°C	100							Samples held over the bath until the temperature gets close to the bath temperature (10 min)	Samples held over the bath until the temperature gets close to the bath temperature		800
	Shape		Cilyndrical		Cilyndrical	Spherical		Cilyndrical		Cilyndrical	Cilyndrical		Cilyndrical
													Square
	Length Total	mm	50,8		300		406	76,2		70	80-120	230	343
	Submerged Length	mm			180-200					55	55-70		170
	Diameter	mm			12,7			12,7		12,0	12,1		
	Diameter	mm	19,1		19,1								25,4
	Diameter	mm			25,4		25,4						31,8
	Diameter	mm			38,1	54							38,1
	Diameter	mm			50,8	79	76,2						
	Side Length (Square)	mm											19,1
	Re-using samples	Y/N					Yes				Yes		
Quenching	Midia				Water						N2	Water	Water

Publishing	**Author**	**R Olsson**	**D Pehlke**	**R Guthrie**	**R Guthrie**	**D Pehlke**	**K Mori**	**J Wright**		**G Brooks**
	Year	1965	1965	1971	1973	1974	1982	1989		2005
	Institution	US Steel Corp	Univ of Michigan	McGill Univ	McGill Univ	Univ of Michigan	Nagoya Univ	CSIRO		McMaster
Heating Furnace	Type		Induction	Induction	Induction	Induction	Resistance-heated	Resistance-heated	Induction		Induction
	Power	kW							40		75
	Temperature control								HP Controller		Manual
	Heating Rate	°C/min							5		
	Thermocouples						Pt/Pt-10%Rh	Pt-Rh			Type-S
	Vertical Tube OD (Resistance Fnce)	mm					88,9	52			
	Capacity	kg	1,2	100	10	250		1	1	25	70
	Crucible material							Graphite	Al2O3-SiOx		MgO
	Crucible length	mm		355	127			125			375
	Crucible Diameter	mm		100	114			40			
	Crucible Thickness	mm									
	Free board	mm									88
	Liquid Height	mm							55 - 70	225	287
Sample and Other Measurements	Weigth Scale	g									+/- 1
	Diameter	mm	"Average Diameter" of all the immersed length was measured	"Average Diameter" of all the immersed length was measured as well volumetric displacement		Weighting and reusing (total cycle 8 sec)		"Average Diameter" measurements	"Average Diameter" estimated from weight loss measurements		"Effective Part", only a same diameter segment of the immersed length was measured
	Temperature		Thermocouple in the center of the sample (Upper part)	Thermocouple in the center of the sample							
	Metallography			Boundary layer showing carbon gradient							
	Off-gas	Flow Rate									
		Chemical composition						Not measured, only estimated			
	Visual Inspection							The liquid near the sample moves downward during dissolution. The lower part is thicker. The opposite occurs when CO bubbling is intense			

Annex 1 – Thermodynamics – Equations and Data Summary

Equilibrium relations in the system Fe-C-O

The liquid solution assumes Henryan behavior for C and O dissolved in Fe

[C]-[O]-CO

Liquid Phase: Solution Fe-C-O

Gas Phase: CO (CO_2 and O_2 neglected)

Fe-C-O as a liquid solution in equilibrium with CO in the gas phase, where total pressure

$p = p_{CO}$

Reaction	Standard Gibbs Free Energy [116] J/mol	
$C_{gr} + 1/2O_{2(g)} \rightarrow CO_{(g)}$	ΔG^0 = -111,700 – 87.65 T	eq.AN1 - 1
$C_{gr} \rightarrow \underline{C}$ 1% wt	ΔG^0 = 22,594 – 42.26 T	eq.AN1 - 2
$1/2O_2 \rightarrow \underline{O}$ 1% wt	ΔG^0 = -115,750 – 4.63 T	eq.AN1 - 3
$\underline{C} + \underline{O} \rightarrow CO_{(g)}$	ΔG^0 = -18,544 – 40.76 T	eq.AN1 - 4

Table AN1 - 1 Expressions for Standard Gibbs Free Energy for C-O reactions. Equilibrium with CO.

$$K_{CO} = \frac{P_{CO}}{h_C.h_O} = EXP\left(\frac{2{,}230}{T} + 4.90\right) \qquad \text{eq.AN1 - 5}$$

Accounting Henryan activity eq.AN1 - 6

$$h_i = f_i.[\%X_i]$$

$$\ln\left(\frac{P_{CO}}{f_C.[\%C].f_O.[\%O]}\right) = \frac{2{,}230}{T} + 4.90 \qquad \text{eq.AN1 - 7}$$

$$[\%C] = \left(\frac{P_{CO}}{f_C \cdot f_O}\right) \cdot EXP\left(-\frac{2{,}230}{T} - 4.90\right) \cdot \frac{1}{[\%O]} \qquad \text{eq.AN1 - 8}$$

$$[\%O] = \left(\frac{P_{CO}}{f_C \cdot f_O}\right) \cdot EXP\left(-\frac{2{,}230}{T} - 4.90\right) \cdot \frac{1}{[\%C]} \qquad \text{eq.AN1 - 9}$$

$$\log f_C = e_C^C.[\%C] + e_C^O.[\%O] \qquad \text{eq.AN1 - 10}$$

$$\log f_O = e_O^O.[\%O] + e_O^C.[\%C] \qquad \text{eq.AN1 - 11}$$

e_C^C	e_C^O	e_O^O	e_O^C
0.14	-0.34	-0.20	-0.13

Table AN1 - 2 Interaction coefficients for dilute solutions of elements dissolved in iron at 1600 °C [116]

[C]-[O]-CO
Note: alternative data

Liquid Phase: Solution Fe-C-O

Gas Phase: CO (CO_2 and O_2 neglected)

Fe-C-O forming a liquid solution in equilibrium with CO in the gas phase, where total pressure $p = p_{CO}$

Reactions	Standard Gibbs Free Energy [116] J/mol	
$*C_{gr} + 1/2O_{2(g)} \rightarrow CO_{(g)}$	ΔG^0 = -114,400 – 85.8 T	eq.AN1 - 12
$C_{gr} \rightarrow \underline{C}$ 1% wt	ΔG^0 = 22,594 – 42.26 T	eq.AN1 - 2
$1/2O_2 \rightarrow \underline{O}$ 1% wt	ΔG^0 = -115,750 – 4.63 T	eq.AN1 - 3
$\underline{C} + \underline{O} \rightarrow CO_{(g)}$	ΔG^0 = -21,244 – 38.91 T	eq.AN1 - 13

Table AN1 - 3 Expressions for Standard Gibbs Free Energy for C-O reactions. Equilibrium with CO. (*) Alternative data base [9]

$$K_{CO} = \frac{P_{CO}}{h_C . h_O} = EXP\left(\frac{2{,}555}{T} + 4.67\right) \qquad \text{eq.AN1 - 14}$$

Accounting Henryan activity eq.AN1 - 15

$$h_i = f_i . [\%X_i]$$

$$\ln\left(\frac{P_{CO}}{f_C . [\%C] . f_O . [\%O]}\right) = \frac{2{,}555}{T} + 4.67 \qquad \text{eq.AN1 - 16}$$

$$[\%C] = \left(\frac{P_{CO}}{f_C \cdot f_O}\right) \cdot EXP\left(-\frac{2{,}555}{T} - 4.67\right) \cdot \frac{1}{[\%O]} \qquad \text{eq.AN1 - 17}$$

$$[\%O] = \left(\frac{P_{CO}}{f_C \cdot f_O}\right) \cdot EXP\left(-\frac{2{,}555}{T} - 4.67\right) \cdot \frac{1}{[\%C]} \qquad \text{eq.AN1 - 18}$$

$$\log f_C = e_C^C . [\%C] + e_C^O . [\%O] \qquad \text{eq.AN1 - 19}$$

$$\log f_O = e_O^O . [\%O] + e_O^C . [\%C] \qquad \text{eq.AN1 - 20}$$

[C]-[O]-CO_2

Liquid Phase: Solution Fe-C-O

Gas Phase: CO-CO_2 (O_2 neglected)

Fe-C-O as a liquid solution in equilibrium with CO and CO_2 in the gas phase, where total pressure $p_{CO} + p_{CO_2} = 1$,

Reactions	Standard Gibbs Free Energy [116] J/mol	
$C_{gr} + 1/2 O_{2(g)} \rightarrow CO_{(g)}$	ΔG^0 = -111,700 – 87.65 T	eq.AN1 - 1
$C_{gr} + O_{2(g)} \rightarrow CO_{2(g)}$	ΔG^0 = -394,100 – 0.84 T	eq.AN1 - 21
$C_{gr} \rightarrow \underline{C}$ 1% wt	ΔG^0 = 22,594 – 42.26 T	eq.AN1 - 2
$CO_{2(g)} + \underline{C} \rightarrow 2CO_{(g)}$	ΔG^0 = 148,006 -132.20T	eq.AN1 - 22

Table AN1 - 4 Expressions for Standard Gibbs Free Energy for C-O reactions. Equilibrium with CO and CO_2

$$K_{CO2} = \frac{P_{CO}^2}{P_{CO_2}.h_C} = EXP\left(\frac{-17{,}802}{T} + 15.90\right) \quad \text{eq.AN1 - 23}$$

Accounting Henryan activity eq.AN1 - 24

$$h_i = f_i.[\%X_i]$$

$$\ln\left(\frac{P_{CO}^2}{P_{CO_2}.f_C.[\%C]}\right) = \frac{17{,}802}{T} + 15.90 \quad \text{eq.AN1 - 25}$$

assuming $P_{CO} + P_{CO_2} = 1$ eq.AN1 - 26

$$\frac{P_{CO}^2}{1 - P_{CO}} = EXP\left(\frac{-17{,}802}{T} + 15.90\right).f_C.[\%C] \quad \text{eq.AN1 - 27}$$

The Henryan activity coefficient is also an exponential function of carbon concentration [117]

$$[\%\underline{C}] < 1\%$$

$$\log f_C = 0.167 \cdot [\%C] \quad \text{eq.AN1 - 28}$$

$$[\%\underline{C}] > 1\%$$

$$\log f_C = 0.200 \cdot [\%C] \quad \text{eq.AN1 - 29}$$

[C]-[O]-CO-(FeO)

Liquid Phase: Solution Fe-C-O

Pure FeO (Slag)

Gas Phase: CO-CO_2-O_2

Fe-C-O as a liquid solution in equilibrium with CO, CO_2 and O_2 in the gas phase, where the activity of FeO is $a_{FeO} = 1$

Reactions	Standard Gibbs Free Energy [116] J/mol	
$Fe_{(l)} + 1/2O_{2(g)} \rightarrow FeO_{(l)}$	ΔG^0 = -256,000 + 53.68 T	eq.AN1 - 30
$1/2O_2 \rightarrow \underline{O}$ 1% wt	ΔG^0 = -115,750 – 4.63 T	eq.AN1 - 3
$Fe_{(l)} + \underline{O} \rightarrow FeO_{(l)}$	ΔG^0 = -140,250 + 58.31 T	eq.AN1 - 31

Table AN1 - 5 Expressions for Standard Gibbs Free Energy for Fe-O reactions. Equilibrium with pure FeO

$$K_{FO} = \frac{a_{FeO}}{h_O} = EXP\left(\frac{16{,}869}{T} - 7.01\right) \qquad \text{eq.AN1 - 32}$$

Assuming $a_{FeO} = 1$

$$\ln h_O = -\frac{16{,}869}{T} + 7.01 \qquad \text{eq.AN1 - 33}$$

rearranging eq.AN1 - 7

$$\ln P_{CO} - \ln f_C.[\%C] - \ln f_O.[\%O] = \frac{2{,}230}{T} + 4.90 \qquad \text{eq.AN1 - 34}$$

Fe saturated with oxygen, precipitating pure FeO

$$\ln h_O = \ln f_O.[\%O] \qquad \text{eq.AN1 - 35}$$

Combining

eq.AN1 - 33 to eq.AN1 - 35

$$[\%C_{MIN}] = EXP\left(\frac{14{,}639}{T} - 11.91 + \ln\frac{P_{CO}}{f_C}\right) \qquad \text{eq.AN1 - 36}$$

$[\%C_{MIN}]$ is the carbon concentration in equilibrium when the maximum oxygen solubility is achieved under $a_{FeO} = 1$

[C]-[O]-CO-(FeO)
Note: alternative data

Liquid Phase: Solution Fe-C-O

Pure FeO (Slag)

Gas Phase: CO-CO_2-O_2

Fe-C-O as a liquid solution in equilibrium with CO, CO_2 and O_2 in the gas phase, where the activity of FeO is $a_{FeO} = 1$

Reactions	Standard Gibbs Free Energy [116] J/mol	
$*\ Fe_{(l)} + 1/2O_{2(g)} \rightarrow FeO_{(l)}$	ΔG^0 = -225,500 + 41.3 T	eq.AN1 - 37
$1/2O_2 \rightarrow \underline{O}$ 1% wt	ΔG^0 = -115,750 – 4.63 T	eq.AN1 - 3
$Fe_{(l)} + \underline{O} \rightarrow FeO_{(l)}$	ΔG^0 = -109,750 + 45.93 T	eq.AN1 - 31

Table AN1 - 6 Expressions for Standard Gibbs Free Energy for Fe-C-O reactions. Equilibrium with CO. (*) Alternative Data base [9]

$$K_{FO} = \frac{a_{FeO}}{h_O} = EXP\left(\frac{13{,}200}{T} - 5.52\right) \qquad \text{eq.AN1 - 38}$$

assuming $a_{FeO} = 1$

$$\ln h_O = -\frac{13{,}200}{T} + 5.52 \qquad \text{eq.AN1 - 39}$$

rearranging eq.AN1 - 7

$$\ln P_{CO} - \ln f_C.[\%C] - \ln f_O.[\%O] = \frac{2{,}555}{T} + 4.67 \qquad \text{eq.AN1 - 40}$$

Fe saturated with oxygen, precipitating pure FeO

$$\ln h_O = \ln f_O.[\%O] \qquad \text{eq.AN1 - 41}$$

Combining eq.AN1 - 39 to eq.AN1 - 41

$$[\%C_{MIN}] = EXP\left(\frac{10{,}645}{T} - 10.19 + \ln\frac{P_{CO}}{f_C}\right) \qquad \text{eq.AN1 - 42}$$

$[\%C_{MIN}]$ is the carbon concentration in equilibrium when the maximum oxygen solubility is achieved under $a_{FeO} = 1$

<C_{gr}>-CO-(FeO)

Liquid Phase: Pure FeO (Slag)

Gas Phase: CO (CO_2 and O_2 are neglected)

Solid Phase: C_{gr} (Pure graphite)

FeO as a liquid solution in equilibrium with CO, CO_2 and O_2 in the gas phase, where the activity of FeO is $a_{FeO} = 1$

Reactions	Standard Gibbs Free Energy [116] J/mol	
$Fe_{(l)} + 1/2O_{2(g)} \rightarrow FeO_{(l)}$	ΔG^0 = -256,000 + 53.68 T	eq.AN1 - 30
$C_{gr} + 1/2O_{2(g)} \rightarrow CO_{(g)}$	ΔG^0 = -111,700 – 87.65 T	eq.AN1 - 1
$FeO_{(l)} + C_{gr} = Fe + CO$	ΔG^0 = 144,300 – 141.33 T	eq.AN1 - 43

Table AN1 - 7 Expressions for Standard Gibbs Free Energy for Fe-C-O reactions. Reduction of FeO with C graphite. Equilibrium with CO.

$$K_{FC\,gr} = EXP\left(-\frac{17{,}356}{T} + 16.99\right) \qquad \text{eq.AN1 - 44}$$

assuming $a_{FeO} = 1$ and $a_{C_{gr}} = 1$

$$K_{FC} = \frac{p_{CO}}{a_{FeO}.h_C} = p_{CO} \qquad \text{eq.AN1 - 45}$$

$$p_{CO} = EXP\left(-\frac{17{,}356}{T} + 16.99\right) \qquad \text{eq.AN1 - 46}$$

[C]-CO-(FeO) and variable Slag Basicity

Liquid Phase: FeO-CaO-MgO-SiO_2-P_2O_5 (Slag)

Gas Phase: CO (CO_2 and O_2 are neglected)

Solid Phase: C_{gr} (Pure graphite)

FeO as a liquid solution in equilibrium with CO in the gas phase. The activity of FeO a_{FeO} is a function of slag basicity.

Reactions	Standard Gibbs Free Energy [116] J/mol	
$Fe_{(l)} + \underline{O} \rightarrow FeO_{(l)}$	ΔG^0 = -140,250 + 58.31 T	eq.AN1 - 31
$\underline{C} + \underline{O} \rightarrow CO_{(g)}$	ΔG^0 = -18,544 – 40.76 T	eq.AN1 - 13
$FeO_{(l)} + \underline{C} = Fe + CO$	ΔG^0 = 121,706 – 99.07 T	eq.AN1 - 47

Table AN1 - 8 Expressions for Standard Gibbs Free Energy for Fe-C-O reactions. Reduction of FeO , equilibrium with CO and variable a_{FeO} as a function of slag basicity..

$$K_{FC} = EXP\left(-\frac{14{,}639}{T} + 11.91\right) \qquad \text{eq.AN1 - 48}$$

$$K_{FC} = \frac{P_{CO}}{a_{FeO}.h_C} = \frac{P_{CO}}{a_{FeO}.f_C.[\%C]} \qquad \text{eq.AN1 - 49}$$

$$a_{FeO} = \gamma_{FeO}.\%X_{FeO} \qquad \text{eq.AN1 - 50}$$

$$\%X_i = \%w_i \frac{\frac{\%w_i}{MW_i}}{\sum \frac{\%w_i}{MW_i}} \qquad \text{eq.AN1 - 51}$$

$$\%X_{FeO} = \frac{\left(\frac{\%w_{FeO}}{MW_{FeO}}\right)}{\sum \frac{\%w_i}{MW_i}} = \frac{w_{FeO}}{MW_{FeO} \cdot \sum \frac{\%w_i}{MW_i}} \qquad \text{eq.AN1 - 52}$$

$$a_{FeO} = \gamma_{FeO}.\frac{\%w_{FeO}}{MW_{FeO} \cdot \sum \frac{\%w_i}{MW_i}} \qquad \text{eq.AN1 - 53}$$

Molecular weight of FeO slag defined as MW_{FeO} and MW_{Slag}, respectively. The slag molecular weight is estimated based on typical slag compositions as presented in

Table AN1 - **9**. Hence, $\sum \frac{\%w_i}{MW_i} \approx 1.64\%/(g/mol)$

Thus, at 1873 K, assuming f_c=1 e P_{CO}=1 atm, where FeO and C are mass concentration

$$K_{FC} = \frac{1}{\gamma_{FeO}.(0{,}00847).(\%FeO).[\%C]} = 59{,}99$$

$$(\%FeO).[\%C] = \frac{1}{\gamma_{FeO}.(0{,}508)} \qquad \text{eq.AN1 - 54}$$

Table AN1 - 9 – Estimate of molar weight of typical EAF slag

	MW_i	% wt Slag	MW_i	% wt Slag	MW_i	% wt Slag	MW_i	% wt Slag
FeO	72	20%	72	15%	72	35%	72	40%
CaO	56	40%	56	45%	56	30%	56	25%
SiO2	60	14%	60	18%	60	15%	60	15%
MgO	40	6%	40	6%	40	10%	40	10%
P2O5	142	2%	142	2%	142	1%	142	1%
Cr2O3	152	2%	152	2%	152	2%	152	2%
Al2O3	102	5%	102	5%	102	2%	102	2%
Other	60	5%	60	5%	60	5%	60	5%
	61,8	94%	63,2	98%	64,5	100%	65,3	100%
Basicity B		3,01		2,71		2,78		2,46

<C_{gr}>-CO-CO_2-(FeO)

Liquid Phase: Pure FeO (Slag)

Gas Phase: CO and CO_2 (O_2 is neglected)

Solid Phase: C_{gr} (Pure graphite)

FeO as a liquid solution in equilibrium with CO, CO_2 and O_2 in the gas phase, where the activity of FeO is $a_{FeO} = 1$

Reactions	Standard Gibbs Free Energy [116] J/mol	
$Fe_{(l)} + 1/2O_{2(g)} \rightarrow FeO_{(l)}$	ΔG^0 = -225,500 + 41.3 T	eq.AN1 - 37
$C_{gr} + 1/2O_{2(g)} \rightarrow CO_{(g)}$	ΔG^0 = -114,400 – 85.8 T	eq.AN1 - 12
$C_{gr} + O_{2(g)} \rightarrow CO_{2(g)}$	ΔG^0 = -395,300 – 0.5 T	eq.AN1 - 55
$FeO_{(l)} + CO = Fe + CO_2$	ΔG^0 = -55,400 + 44.0 T	eq.AN1 - 56

$$K_{FCO_2} = \frac{P_{CO_2}}{a_{FeO} P_{CO}} = EXP\left(\frac{6{,}663}{T} - 5.29\right) \qquad \text{eq.AN1 - 57}$$

assuming $a_{FeO} = 1$

$$K_{FCO_2} = \frac{P_{CO_2}}{P_{CO}} = EXP\left(\frac{6{,}663}{T} - 5.29\right) \qquad \text{eq.AN1 - 58}$$

<C_{gr}>-CO-CO_2 Boudouard Reaction

Reactions	Standard Gibbs Free Energy [116] J/mol	
$C_{gr} + 1/2O_{2(g)} \rightarrow CO_{(g)}$	ΔG^0 = -114,400 – 85.8 T	eq.AN1 - 12
$C_{gr} + O_{2(g)} \rightarrow CO_{2(g)}$	ΔG^0 = -395,300 – 0.5 T	eq.AN1 - 55
$C_{gr} + CO_2 = 2CO$	ΔG^0 = 166,500 -171.1 T	eq.AN1 - 59

$$K_{boud} = \frac{p_{CO}^2}{a_{C_{gr}} p_{CO_2}} = EXP\left(-\frac{20{,}025}{T} + 20.58\right) \qquad \text{eq.AN1 - 60}$$

assuming $a_{C_{gr}} = 1$

$$K_{boud} = \frac{p_{CO}^2}{p_{CO_2}} = EXP\left(-\frac{20{,}025}{T} + 20.58\right) \qquad \text{eq.AN1 - 61}$$

CO-CO_2 Equilibrium in the gas phase

Liquid Phase: None

Gas Phase: CO, CO_2 and O_2

Solid Phase: None

Reactions	Standard Gibbs Free Energy [116] J/mol	
$C_{gr} + 1/2O_{2(g)} \rightarrow CO_{(g)}$	ΔG^0 = -114,400 – 85.8 T	eq.AN1 - 12
$C_{gr} + O_{2(g)} \rightarrow CO_{2(g)}$	ΔG^0 = -395,300 – 0.5 T	eq.AN1 - 55
$CO_{(g)} + 1/2O_{2(g)} \rightarrow CO_{2(g)}$	ΔG^0 = -280,900 + 85.3 T	eq.AN1 - 62

$$K_{CO-CO_2} = \frac{p_{CO_2}}{p_{CO}.p_{O_2}^{1/2}} = EXP\left(-\frac{33{,}786}{T} + 8.31\right) \qquad \text{eq.AN1 - 63}$$

Equilibrium relations in the system Fe-Mn-O

[Fe]- [Mn]-[O]-(FeO)-(MnO)

Liquid Phase: Solution Fe-Mn-O

FeO and MnO (Slag)

Gas Phase: O_2

Fe-Mn-O as a liquid solution in equilibrium with FeO and MnO in the slag phase, where the activity of FeO is $a_{FeO} = 1$

Reactions	Standard Gibbs Free Energy [116] J/mol	
$\underline{Fe} + 1/2O_{2(g)} \rightarrow FeO_{(l)}$	ΔG^0 = -225,500 + 41.3 T	eq.AN1 - 30
$\underline{Mn} + 1/2O_{2(g)} \rightarrow MnO_{(l)}$	ΔG^0 = -356,584 + 100.7 T	eq.AN1 - 64
$FeO_{(l)} + \underline{Mn} \rightarrow MnO_{(l)} + \underline{Fe}$	ΔG^0 = -131,084 + 59.40 T	eq.AN1 - 65

Table AN1 - 10 Expressions for Standard Gibbs Free Energy for Fe-Mn-O reactions. Equilibrium with pure FeO and MnO

$$K_{FeMn} = \frac{a_{MnO}}{a_{FeO}.[\%Mn]} = EXP\left(\frac{15{,}766}{T} - 7.144\right) \qquad \text{eq.AN1 - 66}$$

$$K_{FeMn} = \frac{\gamma_{MnO}X_{MnO}}{\gamma_{FeO}X_{FeO}.[\%Mn]} = EXP\left(\frac{15{,}766}{T} - 7.144\right) \qquad \text{eq.AN1 - 67}$$

$$\frac{\gamma_{FeO}}{\gamma_{MnO}} = \frac{1}{K_{FeMn}} \frac{X_{MnO}}{X_{FeO}.[\%Mn]}$$ eq.AN1 - 68

@1873 K, $K_{FeMn} = 3.57$

According to data cited in Figure 5, eq.AN1 - 68 s plotted in Figure AN1 - 1 (a), a function basicity index $B = \frac{\%CaO + 1.4\%MgO}{\%SiO_2 + 0.84\%P_2O_5}$. Therefore, the Figure AN1 - 1 (b) is derived from eq.AN1 - 68 s plotted in Figure AN1 - 1 (a).

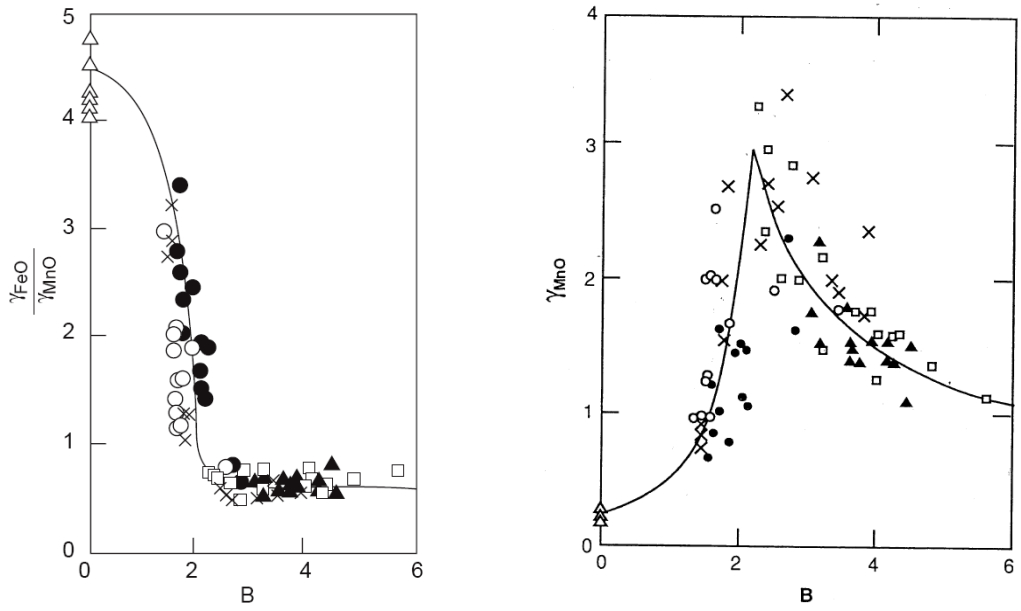

(a) (b)

Figure AN1 - 1 - Variation of activity coefficient ratio $\frac{\gamma_{FeO}}{\gamma_{MnO}}$ with slag Basicity at 1873 K[10]

Regular Solution Model

The excess value of an extensive thermodynamic solution property is the difference between its actual value and the value it would have if the solution was ideal [116].

$$G = G^{id} + G^{XS} \qquad \text{eq.AN1 - 69}$$

G molar Gibbs free energy
G^{id} molar Gibbs free energy if it were ideal solution
G^{XS} excess of molar Gibbs free of the solution

$$\Delta G^{M} = \Delta G^{M,id} + G^{XS} \qquad \text{eq.AN1 - 70}$$

For Raoultian ideal solutions

$$a_i = X_i \qquad \text{eq.AN1 - 71}$$

$$\Delta G^{M,id} = RT(X_A \ln X_A + X_B \ln X_B + ... + X_n \ln X_n) = \\ = \sum X_i \overline{\Delta G_i}^{M,id} \qquad \text{eq.AN1 - 72}$$

$$\overline{\Delta G_i}^{M,id} = RT \ln X_i \qquad \text{eq.AN1 - 73}$$

For Non-ideal Solutions

$$\gamma_i = \frac{a_i}{X_i} \qquad \text{eq.AN1 - 74}$$

$$\overline{G}_i = RT \ln \gamma_i \qquad \text{eq.AN1 - 75}$$

Considering a binary solution

$$G^{XS} = RT\alpha X_A X_B \qquad \text{eq.AN1 - 76}$$

$$RT \ln \gamma_A = \alpha' X_B^2 \qquad \text{eq.AN1 - 77}$$

$$\alpha' = \alpha RT \qquad \text{eq.AN1 - 78}$$

$$G^{XS} = RT\alpha X_A X_B \qquad \text{eq.AN1 - 79}$$

For a multiple species system

$$RT \ln \gamma_i = \sum_j \alpha_{ij} X_j^2 + \sum_j \sum_k (\alpha_{ij} + \alpha_{ik} - \alpha_{ijk}).X_j X_k \qquad \text{eq.AN1 - 80}$$

α_{ij} is the interaction coefficient energy between cation (*i* cation)-O-(*j* cation)
The reference state is taken to hypothetical pure liquid of oxide species [107].

FeO-$FeO_{1.5}$-MnO-SiO_2-MgO-CaO αij

i \ j		XFeO	$XFeO_{1.5}$	XMnO	$XSiO_2$	XMgO	XCaO	XP_2O_5	XAl_2O_3
		Fe^{2+}	Fe^{3+}	Mn^{2+}	Si4 +	Mg2+	Ca2+	p5 +	A13+
XFeO	Fe2+		-18660	7110	-41840	33470	-31380	-31380	-41000
XFeO1.5	Fe3+	18660		-56480	32640	-2930	-95810	14640	- 161 080
XMnO	Mn2+	7110	-56480		-75310	61920	-92050	-84940	- 83 680
XSiO2	Si4+	-41840	32640	-75310		-66940	-133890	83680	-127610
XMgO	Mg2+	33470	-2930	61920	-66940		-100420	-37660	-71130
XCaO	Ca2+	-31380	-95810	-92050	-133890	-100420		-251040	-154810
XP_2O_5	P5+	-31380	14640	-84940	83680	-37660	-251040		-261500
XAl_2O_3	Al3+	-41000	-161080	-83680	-127610	-71130	-154810	-261500	

Table 31 - Interaction energy between cations of major components in steelmaking slag **[107].**

		INPUT	OUTPUT						MW_i Reactant 1	MW_i Product 1	MW_i Product 2	$\frac{a.MW_{Me_i}}{c.MW_{MeO_i}}$	O_2 consumption		Entalphy - ΔH
			METAL			SLAG	DUST	OFF-GAS	g/mol	g/mol	g/mol		$Nm3O_2$/ kg Reactant	$Nm3O_2$/ Nm3 Reactant 1	kWh/kg or Nm3 Reactant
FERROUS MATERIALS	Me_i	C	C	Tapping Carbon				C+1/2O2 -> CO	12,00	28,00			0,933		2,559
								CO+1/2O2->CO2	28,00	44,00				1,000	3,512
	Me_i	Si	Si	Min_{Me}	0,001	Si+O2->SiO2			28,09	60,09		0,467	0,797		9,427
	Me_i	Mn	Mn	L_{Me}		Mn+1/2O2=MnO			54,94	70,94		0,774	0,204		2,019
	Me_i	S	S	L_{Me}		S+O2->SO2			32,07	64,07		0,501	0,698		3,141
	Me_i	P	P	L_{Me}		P2+5/2O2->P2O5			30,97	141,94		0,436	1,808		6,130
	Me_i	Cu	Cu	NR		2Cu+1/2O2=Cu2O			63,55	143,10		0,888	0,176		0,855
	Me_i	Ni	Ni	NR		Ni+1/2O2->NiO			58,69	74,69		0,786	0,191		1,241
	Me_i	Cr	Cr	L_{Me}		2Cr+3/2O2->Cr2O3			51,00	150,00		0,680	0,659		6,321
	Me_i	Sn	Sn	L_{Me}		Sn+1/2O2->SnO			118,71	134,71		0,881	0,094		1,373
	Me_i	Nb	Nb			2Nb+5/2O2->Nb2O5			92,91	265,82		0,699	0,603		1,870
	Me_i	Mo	Mo	L_{Me}		Mo+O2->MoO2			95,94	127,94		0,750	0,233		1,703
	Me_i	V	V	Min_{Me}	0,000	2V+3/2O2->V2O3			50,94	149,88		0,680	0,660		4,002
	Me_i	Al	Al	Min_{Me}	0,000	2Al+3/2O2->Al2O3			26,98	101,96		0,529	1,245		17,491
	Me_i	Zn	Zn	Min_{Me}	0,000	Zn+1/2O2->ZnO			65,39	81,39		0,803	0,171		2,053
	Me_i	Pb	Pb	Min_{Me}	0,000	Pb+1/2O2->PbO			207,20	223,20		0,928	0,054		0,299
	Me_i	Hg	Hg	Min_{Me}	0,000	Hg+1/2O2->HgO			200,59	216,59		0,926	0,056		
	Me_i	N	N	NR					14,00						
	Me_i	Fe	Fe	K_{FeO}		Fe+1/2O2->FeO	Fe->VaporizatioN->FeO		55,85	71,85			0,201		1,318
	MeO_i	Iron-oxides (Fe_xO_y) in the bulk				FeO			71,85						
			Fe	FeO+C->Fe+CO				CO	71,85	55,85	28,00				-0,558
	MeO_i	Rust (FeO)				FeO			71,85						
			Fe	FeO+C->Fe+CO				CO	71,85	55,85	28,00				-0,558
	MeO_i	DRI/HBI - Gangue Total													
	MeO_i	DRI/HBI - (CaO)				CaO			56,08						
	MeO_i	DRI/HBI - (SiO2)				SiO2			60,09						
	MeO_i	DRI/HBI - (Al2O3)				Al2O3			101,96						
		Oil & Greases & Rubber						C+1/2O2 -> CO	12,00	28,00			0,933		2,559
		Paintings & Coatings						CO+1/2O2->CO2	28,00	44,00				1,000	3,512
	MeO_i	Non-metalics (Dirt) Total													
	MeO_i	Si oxides (SiO2)				SiO2			60,09						
	MeO_i	Ca oxides (CaO)				CaO			56,08						
	MeO_i	Al oxides (Al2O3)				Al2O3			101,96						
	MeO_i	Mg oxides (MgO)				MgO			40,31						
	MeO_i	Water							18,00						
SLAG FORMER MATERIALS	MeO_i	CaO				CaO			56,08						
	MeO_i	MgO				MgO			40,31						
	MeO_i	Al2O3				Al2O3			101,96						
	MeO_i	SiO2				SiO2			60,09						
	MeO_i	CO2 - Lime	CaCO3+(Heat)->CaO+CO2					CO2	44,00						-2,500
	MeO_i	CO2 - Dololime	MgCO3+(Heat)->CaO+CO2					CO2	44,00						-2,166
	MeO_i	H2O				H2O									
						S+O2->SO2			32,07	64,07			0,70		3,141
	Me_i	S													
CARBONACEOUS MATERIALS	Me_i	C						C+1/2O2 -> CO	12,00	28,00			0,93		2,559
								CO+1/2O2->CO2	28,00	44,00			0,40		3,512
			FeO+C->Fe+CO												
	Me_i	S	S	L_{Me}		S+O2->SO2				64,07			0,70		
	MeO_i	CaO				CaO									
	MeO_i	MgO				MgO									
	MeO_i	Al2O3				Al2O3									
	MeO_i	SiO2				SiO2									
	MeO_i	H2O						H2O							
GASES	Gas_i	O2 - Lance	O	K_C				O2	32,00						
	Gas_i	O2 - Burners													
	Gas_i	Natural Gas - Burners						CH4+2O2=CO2+2H2O	16,00	44,00	18,00			2,000	9,860

Table AN1 - 11 – Complimentary thermodynamic data for the main reactions

Annex 2 – Kinetics Equations Summary

Basic notation

	Unit	Fraction	Density or Concentration	Flow
Mass	*W* (kg)	*w or wt* (%)	ρ (kg/m^3)	*J* kg/(s.m^2)
Molar	*n* (moles)	*X* (%)	*C* (moles/m^3)	*N* mol/(s.m^2)

Note: in the Annex 1, mass fraction %wt notation will be replaced by % only.

It is usually postulated that the rate of a chemical reaction is proportional to the concentration of the reacting substances. One of the most common and general forms to represent the rate dependence on the concentration is the power law model. The sum of the powers to which the concentration of the reacting atoms or molecules must be raised to determine the rate of reaction, is known of the order of reaction [118]. This concept comes from intuitive knowledge and many times a chemical reaction could not be expressed in such way. The order of reaction results from the rate-controlling mechanism which is determined by the way the atoms regroup and how their chemical bonding are rearranged in the produced substances [119].

The order of reaction is basically determined by experimental observation, and may assume values in the form of integer, fraction, positive, negative, or even null.

The reactants A and B produce C and D

$$A^a + B^b \leftrightarrow C^c + D^d \qquad \text{eq.AN2 - 1}$$

The rate of reaction can be estimated by the power law

$$-r_A = k_A.C_A^a.C_B^b \qquad \text{eq.AN2 - 2}$$

The reaction rate could be writing in terms of reactant activities $C_A^a = (\gamma_A.C_A)^a$, assuming that the coefficient of activities do not change significantly during the progress of reaction,

$$-r_A = k_A^{'}.(\gamma_A.C_A)^a.(\gamma_B C_B)^b = \left(k_A^{'}.\gamma_A{}^a.\gamma_B{}^b\right).C_A^a.C_B^b \qquad \text{eq.AN2 - 3}$$

meaning that

$$k_A = \left(k'_A.\gamma_A{}^a.\gamma_B{}^b\right) \qquad \text{eq.AN2 - 4}$$

Heterogeneous reactions involve more than one phase, and the reactions occur at the interface between the phases. An irreversible reaction is characterized by the fact that it proceeds in only one direction, and ceases only when the reactants are exhausted. A reversible reaction can proceed in either direction, depending on the concentrations of the reactants and the products relative to the equilibrium concentrations. Thus, considering a forward $-r_{A,\,forward}$ and reverse $k_{-A,reverse}$ reaction rates, the net reaction rate eq.AN2 - **7** can be expressed combining eq.AN2 - 5 and eq.AN2 - 6

$$-r_{A,\,forward} = k_A.C_A^a C_B^b; r_{-A} = k_{-A,reverse}.C_C^c.C_D^d \therefore r_{A,net} = r_A + r_{-A} \qquad \text{eq.AN2 - 5}$$

$$r_{A,net} = r_A + r_{-A} \qquad \text{eq.AN2 - 6}$$

$$-r_{A,net} = k_A.(C_A^a C_B^b - \frac{k_{-A}}{k_A}.C_C^c.C_D^d) \therefore K_C = \frac{k_A}{k_{-A}} \qquad \text{eq.AN2 - 7}$$

Hence, if the reaction reaches the equilibrium condition,

$$r_A \cong r_{A,net}(equilibrium) = 0; K_C = \frac{C_C^c.C_D^d}{C_A^a.C_B^b} \qquad \text{eq.AN2 - 8}$$

<u>Considering the decarburization reaction</u>

<u>Zero-Order Model</u>

Assumptions:

The rate does not depend on carbon and oxygen concentrations.

The transfer rate of carbon in the melt is higher than the transfer rate or supply rate of oxygen at surface.

$$\frac{d[\%C]}{dt} = -k_{C,0}[\%C]^a.[\%O]^b = k_{C,0} \quad a = b = 0 \qquad \text{eq.AN2 - 9}$$

Boundary conditions

$$t = 0 \Rightarrow \%C = \%C_0 \qquad \text{eq.AN2 - 10}$$

$$\int_{\%C_0}^{\%C} d[\%C] = -\int_0^t k_{C,0}.dt \qquad \text{eq.AN2 - 11}$$

$$[\%C_0] - [\%C] = k_{C,0}.t \qquad \text{eq.AN2 - 12}$$

$$[\%C] = [\%C_0] - k_{C,0}.t \qquad \text{eq.AN2 - 13}$$

First-Order Model

Assumptions:

The rate depends only on carbon concentration.

The carbon concentration at the transition point is called "Critical Carbon" $[\%C]^{Cr}$.

The transfer rate of carbon in the melt is the limiting process.

There is a minimum carbon concentration, which is in equilibrium at the interface.

$$\frac{d[\%C]}{dt} = -k_{C,1st}[\%C]^a.[\%O]^b \quad a = 1; b = 0 \qquad \text{eq.AN2 - 14}$$

$$\frac{d[\%C]}{dt} = -k_{C,1st}.\left([\%C] - [\%C]^{eq}\right) \qquad \text{eq.AN2 - 15}$$

Boundary conditions

$t = 0 \Rightarrow \%C = \%C_0$

$$\int_{\%C_0}^{\%C} d[\%C] = -\int_0^t k_{C,1st}.\left([\%C] - [\%C]^{eq}\right).dt \qquad \text{eq.AN2 - 16}$$

$$\int_{\%C_0}^{\%C} \frac{d[\%C]}{\left([\%C] - [\%C]^{eq}\right)} = -\int_0^t k_{C,1st}.dt \qquad \text{eq.AN2 - 17}$$

$$\ln\left([\%C] - [\%C]^{eq}\right) = -k_{C,1st}.t + \ln\left([\%C_0] - [\%C]^{eq}\right) \qquad \text{eq.AN2 - 18}$$

But $[\%C] < [\%C]^{Cr} \Rightarrow [\%C_0] = [\%C]^{Cr}$

$$\ln \frac{\left([\%C] - [\%C]^{eq}\right)}{\left([\%C]^{Cr} - [\%C]^{eq}\right)} = -k_{C,1st}.t \qquad \text{eq.AN2 - 19}$$

$$[\%C] = e^{-k_{C,1st}.t} \cdot \left([\%C]^{Cr} - [\%C]^{eq}\right) + [\%C]^{eq} \qquad \text{eq.AN2 - 20}$$

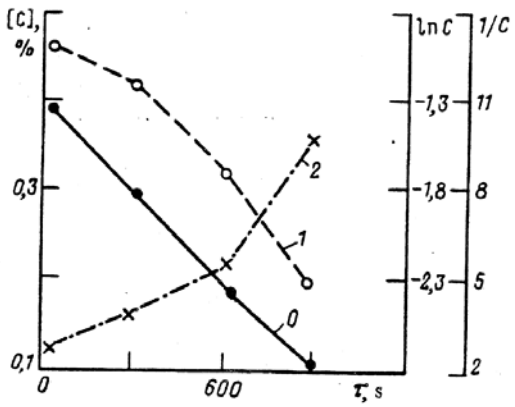

Figure AN2 - 1 – Kinetics curves of variation of carbon concentrations in a 40 ton EAF for process (0) zero, (1) first and (2) second order reactions [30]

Other conversion factors

From eq.AN1 - 22, $CO_{2(g)} + \underline{C} \rightarrow 2CO_{(g)}$

$$N_C = N_{CO_2} \qquad mol/m^2.s$$ eq.AN2 - 21

$$N_C = \frac{dn_C}{dt} = N_{CO_2}$$ eq.AN2 - 22

$$[\%C] = \frac{M_C}{W^{Melt}} = \frac{n_C.MW_C}{\rho^{Melt}.V^{Melt}}$$ eq.AN2 - 23

$$n_C = [\%C]\frac{\rho^{Metal}.V^{Metal}}{MW_C}$$ eq.AN2 - 24

$$\frac{dn_C}{dt} = \frac{d[\%C]}{dt}\frac{\rho^{Metal}.V^{Metal}}{MW_C}$$ eq.AN2 - 25

$$W^{Metal} = \rho^{Metal} \cdot V^{Metal}$$

$$\frac{d[\%C]}{dt} = -\frac{MW_C.A}{W^{Metal}}.N_{CO_2}$$ eq.AN2 - 26

From eq. 17, $2\underline{C} + O_{2_{(g)}} = 2CO_{(g)}$

$$\frac{N_C}{2} = N_{O_2} \qquad mol/m^2.s$$ eq.AN2 - 27

$$N_C = \frac{dn_C}{dt} = 2.N_{O_2}$$ eq.AN2 - 28

$$\frac{dn_C}{dt} = 2.N_{O_2}.A = \frac{\rho^{Melt}.V^{Melt}}{MW_C} \qquad \text{eq.AN2 - 29}$$

$$\frac{d[\%C]}{dt} = -\frac{MW_C.A}{\rho^{Melt}.V^{Melt}}.2.N_{O_2} \qquad \text{eq.AN2 - 30}$$

$$\frac{d[\%C]}{dt} = -\frac{MW_C.A}{W^{Melal}} \cdot 2 \cdot N_{O_2} \qquad \text{eq.AN2 - 31}$$

If some post combustion is assumed to occur as defined in , eq.AN2 - 31 becomes

$$\frac{d[\%C]}{dt} = -\frac{MW_C.A}{W^{Melt}}.(2 - R_{PC}).N_{O_2} \qquad \text{eq.AN2 - 32}$$

Some authors [9] write eq.AN2 - 32 as a function of F_{CO}, which is the fraction of CO in the gas phase. The rest is CO_2.

$$\frac{d[\%C]}{dt} = -\frac{MW_C.A}{W^{Melt}}.(1 + F_{CO}).N_{O_2} \qquad \text{eq.AN2 - 33}$$

Actually, the terms $(2 - R_{PC})$ and $(1 + F_{CO})$ are equal

$$(2 - R_{PC}) = (1 + F_{CO})$$
$$2 - \frac{CO_2}{CO_2 + CO} = 1 + \frac{CO}{CO_2 + CO} \qquad \text{eq.AN2 - 34}$$

Conversing N_{O_2} [mol/time] to $Q_{O_2}.A$ [Nm^3/.time]

$$N_{O_2} \cdot A = \frac{p.Q_{O_2}.A}{RT} = c.Q_{O_2}.A \qquad \text{eq.AN2 - 35}$$

$$c = \frac{p}{RT} = \frac{10^3}{22{,}4} \quad \text{mol/Nm}^3 \qquad \text{eq.AN2 - 36}$$

assuming p = 1 atm, R = 0.082057 E-03 Nm^3.atm/(K.mol),
T = 273 K

Hence, eq.AN2 - 33 can written as

$$\frac{d[\%C]}{dt} = -c.\frac{MW_C}{W^{Melt}}.(1 + F_{CO}).Q_{O_2} \qquad \text{eq.AN2 - 37}$$

From eq.AN3 - 50, $N_{A,S} = m.(C_{A,S} - C_{A,\infty})$

$$N_C = m_C.(C_C^{\infty} - C_C^{eq}) \qquad \text{eq.AN2 - 38}$$

where

C_C is the molar density of carbon [mol/m^3]

$$N_C = \frac{dn_C}{dt} = -\frac{d\left([\%C]\frac{\rho^{Metal}.V^{Metal}}{MW_C}\right)}{dt} = m_C.(C_C^{\infty} - C_C^{eq}) \qquad \text{eq.AN2 - 39}$$

$$\frac{d[\%C]}{dt} = -m_C\frac{MW_C}{W^{Metal}}.A.(C_C^{\infty} - C_C^{eq}) \qquad \text{eq.AN2 - 40}$$

$$\%C = \frac{n_C \cdot MW_C}{W^{Metal}} \qquad \text{eq.AN2 - 41}$$

$$C_C = \frac{n_C}{V^{Metal}} = \frac{n_C \cdot \rho^{Metal}}{W^{Metal}} = \frac{[\%C]\cdot\rho^{Metal}}{MW_C} \qquad \text{eq.AN2 - 42}$$

$$\frac{d[\%C]}{dt} = -\frac{\rho^{Metal}\cdot m_C.A}{W^{Metal}}([\%C]^{\infty} - [\%C]^{eq}) \qquad \text{eq.AN2 - 43}$$

Rate equation for mass transfer of FeO in slag phase

$$N_{FeO} = m_{FeO}.(C_{FeO}^{\infty} - C_{FeO}^{sg}) \qquad \text{eq.AN2 - 44}$$

where m_{FeO} is the mass transfer coefficient of FeO in slag, C_{FeO}^{∞} is molar density of FeO in slag bulk, and C_{FeO}^{i} is the molar density of FeO in interface slag-gas

$$N_{FeO} = \frac{dn_{FeO}}{dt} = -\frac{d\left((\%FeO)\frac{\rho^{Slag}.V^{Slag}}{MW_{FeO}}\right)}{dt} \qquad \text{eq.AN2 - 45}$$

Similarly to carbon mass transport,

$$\frac{d[\%FeO]}{dt} = -\frac{\rho^{Slag}\cdot m_{FeO}.A}{W^{Slag}}((\%FeO)^{\infty} - (\%FeO)^{sg}) \qquad \text{eq.AN2 - 46}$$

or

$$N_{FeO} = \frac{\rho_{Slag}.m_{FeO}}{100.MW_{FeO}}.((\%FeO)^{\infty} - (\%FeO)^{sg}) \qquad \text{eq.AN2 - 47}$$

Considering the FeO reduction reactions

		CHEMICAL RATE CONTROL - INTERFACE	
		Metal-Gas (*ms*)	Slag-Gas (*sg*)
		$C + CO_2 = 2CO$	$FeO + CO = Fe + CO_2$
		$r_{mg} = k_{mg} \cdot [\%C] \cdot p_{CO_2}$	$r_{sg} = k_{mg} \cdot a_{FeO} \cdot p_{CO_2}$
Equilibrium at	Metal-Gas		$K_{FCO} = \frac{p_{CO}^2}{p_{CO_2} \cdot a_C}$
	Slag-Gas	$K_{FCO_2} = \frac{p_{CO_2}}{p_{CO} \cdot a_{FeO}}$	

If the metal-gas reaction is the rate-controlling

$$CO_{2(g)} + \underline{C} \rightarrow 2CO_{(g)}$$

The rate of metal-gas reaction according to eq.AN1 - 22,

$$r_{CO_2} = k_{CO_2}.([\%\underline{C}]^{mg})^{\alpha}.(p_{CO_2}^{mg})^{\beta} \qquad \text{eq.AN2 - 48}$$

assuming $\alpha = 0$, independent of carbon content and $\beta = 1$, $k_{mg} = k_{CO_2}$

Besides, the thermodynamics limit is $p_{CO_2}^{eq} = p_{CO_2}^{sg}$

$$r_{CO_2} = k_{CO_2}.(p_{CO_2}^{sg} - p_{CO_2}^{mg}) \qquad \text{eq.AN2 - 49}$$

it can be assumed that reaction at slag-gas interface $FeO_{(l)} + CO = Fe + CO_2$ is in equilibrium. Therefore,

$$K_{FCO_2} = \frac{p_{CO_2}^{sg}}{a_{FeO} p_{CO}^{sg}} \qquad \text{eq.AN1 - 57}$$

The superscript *sg* means slag-gas interface. Assuming $p_{CO}^{sg} \approx 1$ and according to Boudouard, $p_{CO_2}^{mg}$ is very small [35] ,

$$p_{CO_2}^{sg} = K_{FCO_2} a_{FeO} \qquad \text{eq.AN2 - 50}$$

$$r_{CO_2} = k_{CO_2}.K_{FCO_2}.a_{FeO}$$

considering the activity of FeO being variable

$$a_{FeO} = \gamma_{FeO}.\frac{C_{FeO}}{C_{Slag}} \text{ and } C_{FeO} = [\%FeO]\frac{\rho_{Slag}}{MW_{FeO}}$$

$$r_{CO_2} = \frac{k_{CO_2}.K_{FCO_2}.\gamma_{FeO}.\rho_{Slag}}{100.C_{Slag}.MW_{FeO}}[\%FeO]^{sg} \qquad \text{eq.AN2 - 51}$$

where ρ_{Slag} is the slag density and MW_{FeO} is the molecular weight of FeO

<u>If the slag-gas reaction is the rate-controlling</u>

$$FeO_{(l)} + CO = Fe + CO_2$$

$$r_{CO} = r_{FeO} = r_{CO_2} \qquad \text{eq.AN2 - 52}$$

$$r_{FeO} = k_{CO}.(a_{FeO})^{\alpha}.(p_{CO}^{mg})^{\beta} \qquad \text{eq.AN2 - 53}$$

assuming $\alpha = \beta = 1$, $k_{sg} = k_{CO}$

Besides, the thermodynamics limit is $\left(p_{CO}^{eq}\right)^{mg}$

$$r_{FeO} = k_{CO}.a_{FeO}.(p_{CO}^{mg} - p_{CO}^{sg}) \qquad \text{eq.AN2 - 54}$$

$$p_{CO}^{sg} = \frac{p_{CO_2}^{sg}}{a_{FeO}.K_{FCO_2}} \qquad \text{eq.AN2 - 55}$$

Presuming $p_{CO}^{mg} \approx 1$

$$r_{FeO} = k_{CO}.(1 - \frac{1}{K_{FCO_2}}\frac{p_{CO_2}^{sg}}{a_{FeO}}) \qquad \text{eq.AN2 - 56}$$

and $p_{CO_2}^{sg} \approx 0$ eq.AN2 - 57

$$r_{FeO} \approx k_{sg} \cdot a_{FeO}$$

<u>If the slag-gas reaction and FeO mass transfer is the mixed rate-controlling</u>

If mixed control takes place, chemical reaction rate eq.AN2 - 47 and mass transfer rate eq.AN2 - 50 are equated $N_{FeO} = r_{CO_2}$, resulting in

$$[\%FeO]^{sg} = \frac{\frac{\rho_{Slag}.m_{FeO}}{MW_{FeO}}.[\%FeO]^{\infty}}{\frac{k_{CO_2}.K_{FCO_2}.\gamma_{FeO}.\rho_{Slag}}{100.C_{Slag}.MW_{FeO}} + \frac{\rho_{Slag}.m_{FeO}}{100.MW_{FeO}}}$$ eq.AN2 - 58

Inserting

$$N_{FeO} = \frac{1}{\frac{100.MW_{FeO}}{\rho_{Slag}.m_{FeO}} + \frac{100.C_{Slag}.MW_{FeO}}{k_{CO_2}.K_{FCO_2}.\gamma_{FeO}.\rho_{Slag}}}[\%FeO]^{\infty}$$ eq.AN2 - 59

$$N_{FeO} = k_0.[\%FeO]^{\infty}$$ eq.AN2 - 60

where k_0 is the overall rate constant

$$k_0 = \frac{1}{\frac{100.MW_{FeO}}{\rho_{Slag}.m_{FeO}} + \frac{100.C_{Slag}.MW_{FeO}}{k_{CO_2}.K_{FCO_2}.\gamma_{FeO}.\rho_{Slag}}}$$ eq.AN2 - 61

Carbon dissolution in metal phase

Assumptions: carbon mass transfer through the liquid boundary layer adjacent to carbonaceous material; carbonaceous materials is in spherical geometry; shrinking core model [93] (Figure AN2 - 2); no ash layer formation.

$$N_{C_{gr}} = -\frac{1}{A_t}\cdot\frac{dn_{C_{gr}}}{dt} =$$
$$= N_C = -\frac{1}{A_t}\cdot\frac{dn_C}{dt} = -m_C\cdot\left(C_C^{Sat} - C_C\right)$$ eq. 205

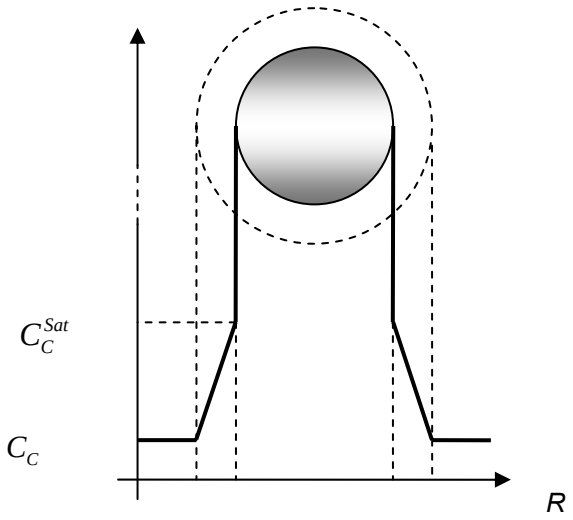

Figure AN2 - 2 – Shrinking core model for carbon dissolution in Fe-C melts. C_C and C_C^{Sat} are the molar concentration in the bulk at any time t and the saturation, respectively.

Sphere

$$N_C = -\frac{1}{4\pi r^2}\cdot\frac{dn_{C_{gr}}}{dt} = -m_C\cdot\left(C_C^{Sat} - C_C\right) \qquad \text{eq.AN2 - 62}$$

$$dn_{C_{gr}} = \frac{\rho^{gr}}{MW_C}.dV^{gr} = \frac{\rho^{gr}}{MW_C}.d\left(\frac{4}{3}\pi r^3\right) = \frac{\rho^{gr}}{MW_C}.4\pi r^2 \qquad \text{eq.AN2 - 63}$$

Combining

$$N_C = -\frac{1}{4\pi r^2}\cdot\frac{\rho^{gr}}{MW_C}.4\pi r^2\frac{dr}{dt} = -m_C\cdot\left(C_C^{Sat} - C_C\right) \qquad \text{eq.AN2 - 64}$$

Integrating

$$-\int_{R_0}^{R_t}\frac{\rho^{gr}}{MW_C}dr = -\int_0^t m_C\cdot\left(C_C^{Sat} - C_C\right)dt \qquad \text{eq.AN2 - 65}$$

$$\frac{\rho^{gr}}{MW_C}.\left(R_0 - R_t\right) = m_C\cdot\left(C_C^{Sat} - C_C\right)t \qquad \text{eq.AN2 - 66}$$

$$W_t^{gr} = \frac{4}{3}\pi R_t^3.\rho^{gr} \qquad \text{eq.AN2 - 67}$$

$$R_t = \left(\frac{3}{4\pi}.\rho^{gr}\right)^{1/3} \qquad \text{eq.AN2 - 68}$$

$$W_t^{gr\,1/3} - W_0^{gr\,1/3} = \frac{\left(\frac{4}{3}\pi\right)^{1/3}}{\rho^{gr\,2/3}} . m_C \cdot MW_C . \left(C_C^{Sat} - C_C\right) . t \qquad \text{eq.AN2 - 69}$$

$$n_C = [\%C] \cdot \frac{W^{Melt}}{MW_C} \qquad \text{eq.AN2 - 70}$$

$$C_C = \frac{n_C}{W^{Melt} / \rho^{Melt}} = [\%C] \cdot \frac{\rho^{Melt}}{MW_C} \qquad \text{eq.AN2 - 71}$$

Combining in terms of particle weight

$$W_t^{gr\,1/3} - W_0^{gr\,1/3} = \frac{\left(\frac{4}{3}\pi\right)^{1/3}}{\rho^{gr\,2/3}} \rho^{Melt} . m_C \cdot \left(\frac{[\%C]_{Sat} - [\%C]_t}{100}\right) . t \qquad \text{eq.AN2 - 72}$$

Combining in terms of mass concentration

$$\frac{1}{A_t} \cdot \frac{W^{Melt}}{MW_C} \frac{d[\%C]}{dt} = m_C \cdot \frac{\rho^{Melt}}{MW_C} \cdot \left(\frac{[\%C]_{Sat} - [\%C]_t}{100}\right) \qquad \text{eq.AN2 - 73}$$

$$\frac{d[\%C]}{dt} = m_C \cdot \frac{\rho^{Melt} A_t}{W^{Melt}} \cdot \left(\frac{[\%C]_{Sat} - [\%C]_t}{100}\right) \qquad \text{eq.AN2 - 74}$$

$$\frac{d[\%C]}{dt} = m_C \cdot \frac{\rho^{Melt} 4\pi \cdot R_t^2}{W^{Melt}} \cdot \left(\frac{[\%C]_{Sat} - [\%C]_t}{100}\right) \qquad \text{eq.AN2 - 75}$$

$$R_t = R_0 - m_C \cdot \frac{\rho^{Melt}}{\rho^{gr}} \cdot \left(\frac{[\%C]_{Sat} - [\%C]_t}{100}\right) . t \qquad \text{eq.AN2 - 76}$$

$$\left.\frac{d[\%C]_t}{dt}\right|_{\mathrm{Re}\,C} = r_t^{\mathrm{Re}\,C} = m_C \cdot \frac{A}{V} \cdot \left(\frac{[\%C]_{Sat} - [\%C]_t}{100}\right) \qquad \text{eq.AN2 - 77}$$

$$\left.\frac{d[\%C]_t}{dt}\right|_{\mathrm{Re}\,C} = \left.\frac{d[W_p]_t}{dt}\right|_{\mathrm{Re}\,C} = \frac{m_C \cdot \rho^{Melt} \cdot A_t}{W^{Melt}} \cdot \left(\frac{[\%C]_{Sat} - [\%C]_t}{100}\right) \quad \text{eq.AN2 - 78}$$

$$W_{p,t} = \left(W_i^{1/3} - \left(\frac{Y}{\rho^{gr}}\right)^{2/3} \cdot \rho^{Melt}.m_C \cdot \left(\frac{[\%C]_{Sat} - [\%C]_t}{100}\right).t \right)^3 \quad \text{eq.AN2 - 79}$$

$$Y = \left(\frac{4}{3}\pi\right)^{1/2} \quad \text{eq.AN2 - 80}$$

Data [92]

ρ_S	1,6	g/cm^3
ρ_L	7,0	g/cm^3
Y	2,047	geometrical cte
m_C	0,12	cm/s
%Csat	5,0%	
%C	0,1%	

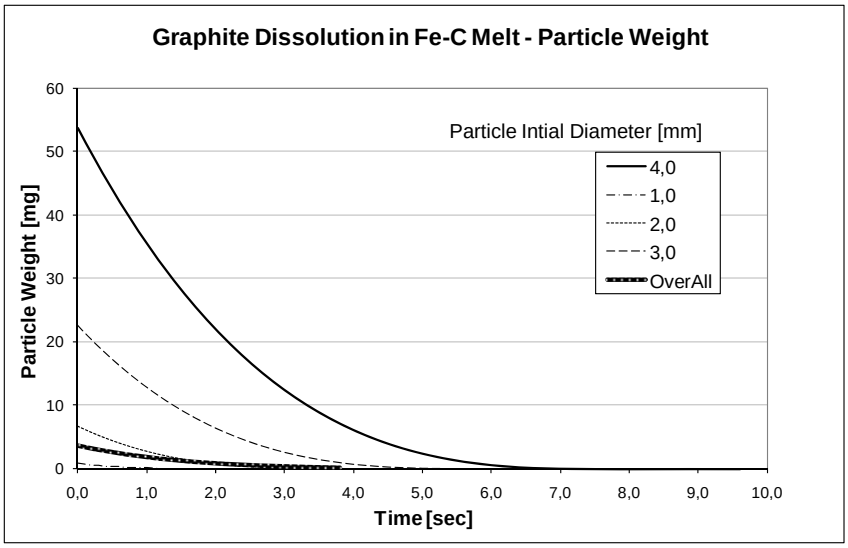

Figure AN2 - 3 – Carbonaceous materials weight loss during dissolution in metal phase (size distribution Diameter/%: 0.5/50%; 1.0/25%; 2.0/18%; 3.0/5%; 4.0/2%)

For calculation convenience, recarburization rate is conducted in terms of conversion rate as a function of time

$$Conversion = F_t^{CMatCh} = \frac{W_i - W_{p,t}}{W_i} =$$

$$= \frac{W_i - \left(W_i^{1/3} - \left(\frac{Y}{\rho^{gr}}\right)^{2/3} \cdot \rho^{Melt}.m_C \cdot (\%C_{Sat} - \%\underline{C}).t \right)^3}{W_i} \quad \text{eq.AN2 - 81}$$

Annex 3 – Transport Phenomena – Equations Summary

The supplementary information content in this annex summarizes several concepts and assumptions on transport phenomena fundamentals mentioned along the thesis text.

The three fundamental physical laws:

A.1. Conservation of Mass (continuity equation)

$$\frac{d\rho}{dt}+\vec{\nabla}(\rho.\vec{\vartheta})=\frac{d\rho}{dt}+\frac{\partial(\rho.u)}{\partial x}+\frac{\partial(\rho.v)}{\partial y}+\frac{\partial(\rho.w)}{\partial z}=0 \qquad \text{eq.AN3 - 1}$$

$[kg/s.m^3]$

Assuming incompressible fluid ρ constant, unitary dimension in z-direction

$$\frac{\partial u}{\partial x}+\frac{\partial v}{\partial y}=0 \qquad \text{eq.AN3 - 1}$$

A.2. Newton's 2nd Law of Motion (momentum theorem)

$$\sum\frac{\vec{F}}{V}=\frac{d(\vec{\rho})}{dt}=\vec{v}.\frac{d(\rho)}{dt}+\rho\frac{d(\vec{v})}{dt}=\rho.\frac{d(\vec{v})}{dt} \qquad \text{eq.AN3 - 2}$$

$$\sum\frac{\vec{F}}{V}=\rho\vec{g}-\vec{\nabla}.P+\vec{R}+\vec{f}_{\mu} \qquad \text{eq.AN3 - 3}$$

$$\rho\frac{D\vec{v}}{Dt}=\rho\left[\frac{d\vec{\vartheta}}{dt}+u\frac{d\vec{\vartheta}}{dx}+v\frac{d\vec{\vartheta}}{dy}+w\frac{d\vec{\vartheta}}{dz}\right]=\rho\vec{g}-\vec{\nabla}.P+\vec{R}++\vec{f}_{\mu} \qquad \text{eq.AN3 - 4}$$

where ρ is constant, $\vec{v}$ is the fluid velocity, $\vec{F}$ is the inertial forces due to the variation of the momentum acting on the fluid. The forces acting on the volume are: $\rho.\vec{g}$ the gravitational force, and $\vec{R}$ is the reacting force of the surface of the fluid. The forces acting on the surface are $\vec{\nabla}P$ which is due to the static pressure, and $\vec{f}_{\mu}$ is the shear stress due to viscous fluid properties. Assuming there are no forces acting on z-direction and the gravitational and $\vec{R}$ force are negligible, and there is a steady-state condition.

On the x direction

$$f_{\mu,x} = \frac{\partial \tau_{xx}}{\partial x} + \frac{\partial \tau_{yx}}{\partial x} + \frac{\partial \tau_{zx}}{\partial x} \qquad \text{eq.AN3 - 5}$$

$$\vec{f}_{\mu} = \vec{\nabla} \bullet \tau = \vec{\nabla}(-\mu.\vec{\nabla}\vec{v}) = -\mu\vec{\nabla}^2\vec{v} \qquad \text{eq.AN3 - 6}$$

$$\rho\left[\frac{\partial u}{\partial t} + u\frac{du}{dx} + v\frac{du}{dy} + w\frac{du}{dz}\right] = \qquad \text{eq.AN3 - 7}$$

$$\rho g_x - \left(\frac{\partial P}{\partial x} + \frac{\partial P}{\partial y} + \frac{\partial P}{\partial z}\right) + \mu\left(\frac{\partial^2 u}{\partial x^2} + \frac{\partial^2 u}{\partial y^2} + \frac{\partial^2 u}{\partial z^2}\right)$$

Assumptions:

Flow dimension: 2D (x-y) (length and width >>thickness); $\frac{\partial()}{\partial z} = 0$; $w = 0$;

Steady-State: $\frac{\partial()}{\partial t} = 0$

Gravity vertical only: $g_x = 0$

Constant Pressure: $\partial P \equiv 0$

Developed flow: (length>>thickness): $\frac{\partial()}{\partial x} = 0 = \frac{\partial^2 u}{\partial x^2} << \frac{\partial^2 u}{\partial y^2}$

Constant thermo physical properties: ρ, μ

$$\rho\left[v\frac{du}{dy}\right] = \mu\left(\frac{\partial^2 u}{\partial y^2}\right) \qquad \text{eq.AN3 - 8}$$

A.3. 1st Law of Thermodynamics (energy equation)

$$\frac{dE}{dt} = \frac{\delta Q}{dt} - \frac{\delta W_S}{dt} = \frac{\partial}{\partial t}\iiint_{VC} e.\rho.dV + \iint_{SC} \rho.(e + \frac{P}{\rho}).(\vec{v}.d\vec{A}) + \frac{\delta W_{\mu}}{dt} \qquad \text{eq.AN3 - 9}$$

Where $\frac{\delta Q}{dt}$ is energy rate input from an external source, $\frac{\delta W_S}{dt}$ is the work rate done by the fluid on the surroundings. On the right side, $\frac{\partial}{\partial t}\iiint_{VC} e.\rho.dV$ is the accumulated energy rate, $\iint_{SC} \rho.(e + \frac{P}{\rho}).(\vec{v}.d\vec{A})$ is the net energy rate due to the fluid motion and $\frac{\delta W_{\mu}}{dt}$ the viscous energy rate due to shear stress work done by the fluid on the surroundings.

The general energy equation derivation leads to eq.AN3 - 10:

$$\rho.c_p.\frac{DT}{Dt} = k\nabla^2 T + \frac{DP}{Dt} + \mu\Phi + \dot{q} \qquad \text{eq.AN3 - 10}$$

where k is thermal conductivity assumed constant, $\frac{DP}{Dt}$ pressure gradient negligible, $\mu\Phi$ is the viscous dissipation and $\dot{q}$ the internal energy rate generation considered zero.

The left side of eq.AN3 - 10 is the net energy rate which is leaving the control volume due to the overall fluid motion (advection). The right side considers: (i) the net input of energy rate due to heat transfer by conduction in y-direction; (ii) the viscous dissipation which is the net rate of work done by the fluid which is converted irreversibly to thermal energy due to viscous effects in the fluid; (iii) chemical reaction, electrical energy rate, etc.

$$\mu\Phi = \mu\left\{\left(\frac{\partial u}{\partial y} + \frac{\partial v}{\partial x}\right)^2 + 2.\left[\left(\frac{\partial u}{\partial x}\right)^2 + \left(\frac{\partial v}{\partial y}\right)^2\right]\right\} \qquad \text{eq.AN3 - 11}$$

Assumptions

Flow dimension: 2D (x-y) (length and width >>thickness); $\frac{\partial()}{\partial z} = 0$; $w = 0$;

Steady-State: $\frac{\partial()}{\partial t} = 0$

No heat generated: $\dot{q} = 0$

Constant Pressure: $\partial P \equiv 0$

Constant thermo physical properties: ρ, μ

$$\rho.c_p.\left(u\frac{\partial T}{\partial x} + v\frac{\partial T}{\partial y}\right) = k.\left(\frac{\partial^2 T}{\partial x^2} + \frac{\partial^2 T}{\partial y^2}\right) + \qquad \text{eq.AN3 - 12}$$
$$+ \mu\left\{\left(\frac{\partial u}{\partial y} + \frac{\partial v}{\partial x}\right)^2 + 2.\left[\left(\frac{\partial u}{\partial x}\right)^2 + \left(\frac{\partial v}{\partial y}\right)^2\right]\right\}$$

Developed flow: (length>>thickness): $\frac{\partial()}{\partial x} = 0$ $\frac{\partial^2 T}{\partial x^2} << \frac{\partial^2 T}{\partial y^2}$

$$u\frac{\partial T}{\partial x} + v\frac{\partial T}{\partial y} = \alpha\frac{\partial^2 T}{\partial y^2} + \frac{\mu}{\rho.c_p}\left(\frac{\partial u}{\partial y}\right)^2 \qquad \text{eq.AN3 - 13}$$

Heat Transfer

Heat conduction (incompressible fluid, no fluid motion, isobaric and all heat transfer is by conduction)

$c_v \cong c_p$ and the materials thermal properties are regarded to be temperature-independent. From general eq.AN3 - 10

$$\rho.c_p.\frac{\partial T}{\partial t} = \nabla.k\nabla T + \dot{q} \qquad \text{eq.AN3 - 14}$$

$$\frac{\partial T}{\partial t} = \alpha.\nabla^2 T + \frac{\dot{q}}{\rho.c_p} \therefore \alpha = \frac{k}{\rho.c_p} \qquad \text{eq.AN3 - 15}$$

Assuming $\dot{q} = 0$

$$\frac{\partial T}{\partial t} = \alpha.\nabla^2 T \therefore \alpha = \frac{k}{\rho.c_p} \qquad \text{eq.AN3 - 16}$$

Rectangular Coordinates x-y-z (Plates)

$$\frac{\partial T}{\partial t} = \alpha.\left(\frac{\partial^2 T}{\partial x^2} + \frac{\partial^2 T}{\partial y^2} + \frac{\partial^2 T}{\partial z^2}\right) \qquad \text{eq.AN3 - 17}$$

For 1-D case $\frac{\partial}{\partial y} = \frac{\partial}{\partial y} = 0$

$$\frac{\partial T}{\partial t} = \alpha.\left(\frac{\partial^2 T}{\partial x^2}\right) \qquad \text{eq.AN3 - 18}$$

Cylindrical Coordinates r-θ-z (Cylinders)

$$\frac{\partial T}{\partial t} = \alpha.\left(\frac{\partial^2 T}{\partial r^2} + \frac{1}{r}\frac{\partial T}{\partial r} + \frac{1}{r^2}\frac{\partial^2 T}{\partial \theta^2} + \frac{\partial^2 T}{\partial z^2}\right) \qquad \text{eq.AN3 - 19}$$

For 1-D case $\frac{\partial}{\partial \theta} = \frac{\partial}{\partial z} = 0$

$$\frac{\partial T}{\partial t} = \alpha.\left(\frac{\partial^2 T}{\partial r^2} + \frac{1}{r}\frac{\partial T}{\partial r}\right) \qquad \text{eq.AN3 - 20}$$

Spherical Coordinates r-θ-ϕ (Spheres)

$$\frac{\partial T}{\partial t} = \alpha.\left(\frac{1}{r^2}\frac{\partial}{\partial r}\left(r^2\frac{\partial T}{\partial r}\right) + \frac{1}{r^2.\sin\theta}\frac{\partial}{\partial \theta}\left(\sin\theta.\frac{\partial T}{\partial \theta}\right) + \frac{1}{r^2.\sin^2\theta}\frac{\partial^2 T}{\partial \theta^2}\right) \qquad \text{eq.AN3 - 21}$$

For 1-D case $\frac{\partial}{\partial \theta} = \frac{\partial}{\partial \phi} = 0$

$$\frac{\partial T}{\partial t} = \alpha.\left(\frac{1}{r^2}\frac{\partial}{\partial r}\left(r^2\frac{\partial T}{\partial r}\right)\right) = \alpha.\left(\frac{1}{r^2}\left(2.r\frac{\partial T}{\partial r} + r^2\frac{\partial^2 T}{\partial r^2}\right)\right) = \qquad \text{eq.AN3 - 22}$$

$$\alpha.\left(\frac{\partial^2 T}{\partial r^2} + \frac{2}{r}\frac{\partial T}{\partial r}\right)$$

Grouping eq.AN3 - 18, eq.AN3 - 20, eq.AN3 - 22

$$\frac{\partial T}{\partial t} = \alpha.\left(\frac{\partial^2 T}{\partial \xi^2} + \frac{1}{\xi}\frac{\partial T}{\partial \xi}\right) \qquad \text{eq.AN3 - 23}$$

ξ = *x* or *r*

Boundary Layer Principles

Laminar Flow

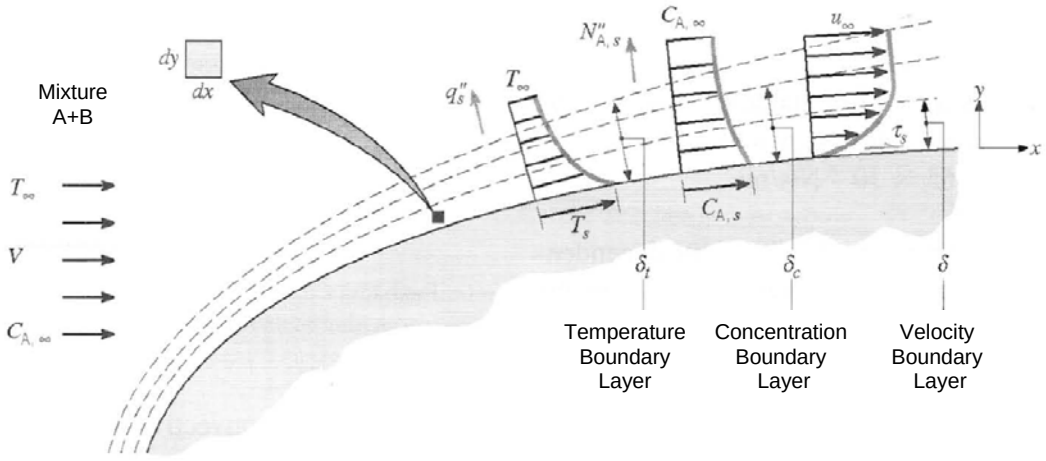

Figure AN- 1 – Development of temperature, concentration and velocity boundary layers for a generic surface [120]

Velocity Boundary Layer

The fluid velocity is zero at the solid surface due to friction effect. The fluid layer above y=0 experiments some velocity losses due to viscous effects. The boundary layer limit $y = \delta$ is defined when the friction effects of the surface on the fluid does not affect significantly the fluid velocity. Arbitrarily, δ is defined where $u = 0.99u_\infty$. Hence, the fluid flow characteristics are composed by two different regions: (i) a thin layer or boundary layer where the velocity and shear stress gradients are significant, and (ii) a region out of the boundary layer where the velocity and shear stress gradients are negligible.

Friction Coefficient

$$C_f \equiv \frac{\tau_s}{\rho.u_\infty^2/2} \qquad \text{eq.AN3 - 24}$$

where ρ and v_∞ are the density and velocity of the fluid at its bulk far from the boundary layer. τ_s is the shear stress acting by the fluid on the surface

Shear Stress

$$\tau_S = \mu.\left.\frac{\partial u}{\partial y}\right|_{y=0} \qquad \text{eq.AN3 - 25}$$

where μ is the fluid viscosity, valid for Newtonian fluids.

Temperature Boundary Layer

The concepts mentioned for the velocity boundary layer are similar to the ones applied to the temperature boundary layer. When the fluid and the surface present different temperatures, a temperature gradient is developed across the fluid from the starting position on the surface. It is assumed that the fluid particles in contact with the surface reach the thermal equilibrium between both phases, keeping the same interface temperature along the heat transfer process. The temperature gradient is developed in the boundary layer defined as $\delta_T = 0.99\frac{(T_S - T_\delta)}{(T_S - T_\infty)}$.

Fourier Law for the fluid (Heat Transfer by Conduction)

$$q_S^{"} = -k_f \left.\frac{\partial T}{\partial y}\right|_{y=0} \qquad \text{eq.AN3 - 26}$$

where k_f is the heat conductivity of the fluid. It is assumed that there is no any fluid motion at $y = 0$, and the heat transfer occurs only by conduction.

Newton's Law for the fluid (Heat Transfer by Convection)

$$q_S^{"} = h.(T_S - T_\infty) \qquad \text{eq.AN3 - 27}$$

where h is the heat transfer coefficient.

Combining eq.AN3 - 71 and eq.AN3 - 69,

$$q_S^{"} = -k_f \left.\frac{\partial T}{\partial y}\right|_{y=0} = h.(T_S - T_\infty)$$

eq.AN3 - 28

$$h = \frac{-k_f \left.\frac{\partial T}{\partial y}\right|_{y=0}}{(T_S - T_\infty)} \equiv \frac{k_f\big|_{y=\delta_T}}{\delta_T}$$

where

$$\left.\frac{\partial T}{\partial y}\right|_{y=\delta_T} \equiv \frac{(T_\infty - T_S)}{\delta_T}$$

When *x* increases the temperature gradient $\frac{\partial T}{\partial y}$ decreases. Considering $(T_S - T_\infty)$ constant, consequently, h and $q_S^{"}$ shall decrease too.

Concentration Boundary Layer

Considering a binary flow mixture of A and B, if there is any concentration gradient from the surface and the fluid, mass transfer is expected to occur. The concentration of A at the surface is considered the thermodynamic equilibrium. The similarity of mass transfer and heat transfer, leads to define

$$\delta_C = 0.99 \frac{(C_{A,S} - C_A)}{(C_{A,S} - C_{A,\infty})}$$

Fick's 1st Law (Diffusion)
Media composed by two species: A and B, stagnant fluid

Mass density

$$\rho_i = \frac{M_i}{V} \quad [kg/m^3]$$

Molar density

$$C_i = \frac{n_i}{V} \quad [mol/m^3]$$

Mass fraction

$$\rho_i = \frac{M_i}{V}$$

Molar fraction

$$X_i = \frac{C_i}{C} = \frac{n_i/V}{\sum n_i/V}$$

Molar flux (1D)

eq.AN3 - 29

$$N_{A,S}^{"} = -D_{AB} \left.\frac{\partial C_A}{\partial y}\right|_{y=0} \qquad [mol/s.m^2]$$

For isothermal and isobaric system, D_{AB} is the mass diffusivity $\left[m^2/s\right]$, or binary diffusivity coefficient of A in the mixture A+B, $C_{A,S}$ is the concentration of specie A ate the interface (subscript *S*). At any position in the boundary layer $0 < y < \delta_C$, the mass transfer shall occur due to the global motion of the fluid

(advection) and diffusion. However, at $y = 0$, there is no fluid motion, and so, the mass transfer is expected to take place only by diffusion.

The diffusivity coefficient was first related as a function of temperature by Einstein

$$D = B.k_B.T \qquad \text{eq.AN3 - 30}$$

k_B is the Boltzman constant

The mass capacity to move is influenced by a potential field, B is defined as the mobility

$$\overline{\vartheta} = B.\overline{F} \qquad \text{eq.AN3 - 31}$$

where $\overline{\vartheta}$ is mean velocity of particles in movement caused by the potential gradient, the force $\overline{F}$.

$$N''_{A,S} = -C_i.\overline{\vartheta} = -C_i.B.\overline{F} \qquad \text{eq.AN3 - 32}$$

$\overline{F} = \nabla V$ where ∇V is the potential gradient, that could be a chemical potential gradient, thus , influence by C_i, γ, a, p, T

In x-direction

$$N''_{A,S} = -C_i.B_i.\frac{\partial V_x}{\partial x} = -C_i.B_i.\frac{\partial(\mu_i^0 + R.T\ln\gamma_i.C_i)}{\partial x} \qquad \text{eq.AN3 - 33}$$

For an ideal mixing, $\gamma_i = 1$

$$N''_{A,S} = -C_i.B_i.R.T\frac{\partial(\ln C_i)}{\partial x} = -C_i.B_i.R.T\frac{1}{C_i}\frac{\partial C_i}{\partial x} = \qquad \text{eq.AN3 - 34}$$

$$= -B_i.R.T\frac{\partial C_i}{\partial x}$$

$$D_i = B_i.R.T \qquad \text{eq.AN3 - 35}$$

Diffusion is an activated process and particles are assumed to jump around their positions due to thermal vibrations. In solids D was derivate in terms of jump frequency Γ and the inter-atomic spacing λ and c coordination number (6, 8 , 12,..)

$$D = \frac{\Gamma\lambda^2}{c} = D_0.e^{-E/RT} \qquad \text{eq.AN3 - 36}$$

$$\Gamma = const.e^{-E/RT} \qquad \text{eq.AN3 - 37}$$

where *E* (activation energy) represents energy barrier to atoms jumping

The diffusion phenomena in liquids cannot be simply extrapolated from diffusion in solids, due to natural convection and experimental problems. However, Eyring theory could be applied to liquid diffusion, assuming that the migrating atoms move from hole to hole by jumping, as initially proposed for solids [41]. Hydrodynamics theory also suggested that diffusivity shall be inversely proportional to the viscosity.

$$D = \frac{k_B.T}{2.R.\mu} \qquad \text{eq.AN3 - 38}$$

where *R* is the radius of the moving sphere particles in a non-reacting and steady-state velocity fluid flow.

Viscosity of liquids was found to behave such as an Arrhenius type equation

$$\mu = A.e^{(1000.B/T)} \qquad \text{eq.AN3 - 39}$$

where *A* and *B* are empirical constants.

When fluid is assumed to be in motion

Generalized Fick's 1st Law (Diffusion)

Media composed by two species: A and B, bulk flow

Molar flux

$$\vec{N}_A = -D_{AB}\nabla C_A + X_A\left(\vec{N}_A + \vec{N}_B\right) \qquad \text{eq.AN3 - 40}$$

where, the bulk motion of specie A is

$$\vec{N}_A = C_A.\vec{\vartheta}_A \qquad \text{eq.AN3 - 41}$$

$D_{AB}\nabla C_A$ portion transported by diffusion (Fick's Law)

$X_A\left(\vec{N}_A + \vec{N}_B\right)$ portion transported by convection

Material flux

$$\frac{\partial (n_A/V)}{\partial t} = \frac{\partial C_A}{\partial t} \qquad [moles/m^3.s]$$

Mass Continuity Equation (moving fluids)

Specie A

$$\vec{\nabla}.\vec{N}_A + \frac{\partial C_A}{\partial t} - R_A = 0$$

Mass Continuity Equation (moving fluids)

Species A and B

$$\vec{\nabla}.(\vec{N}_A + \vec{N}_B) + \frac{\partial (C_A + C_B)}{\partial t} - (R_A + R_B) = 0 \qquad \text{eq.AN3 - 42}$$

$$\vec{N} = C.\vec{\vartheta}$$
$$\vec{\nabla}.\vec{N} = \vec{\nabla}(C.\vec{\vartheta}) = C\vec{\nabla}.\vec{\vartheta} + \vec{\vartheta}.\vec{\nabla}C \qquad \text{eq.AN3 - 43}$$

$$C\vec{\nabla}.\vec{\vartheta} + \left(\vec{\vartheta}.\vec{\nabla}C + \frac{\partial C}{\partial t}\right) - (R_A + R_B) = 0 \qquad \text{eq.AN3 - 44}$$

For specie A

Cylindrical coordinates

$$\vec{\vartheta}.\vec{\nabla}C_A = \left(u\frac{\partial C_A}{\partial x} + v\frac{\partial C_A}{\partial y} + w\frac{\partial C_A}{\partial z}\right) \qquad \text{eq.AN3 - 45}$$

$$\vec{\vartheta} = \vec{\vartheta}(x, y, z) \Rightarrow v_x = u; v_y = v; v_x = w$$

$$\vec{\vartheta}.\vec{\nabla}C_A + \frac{\partial C_A}{\partial t} = \left(u\frac{\partial C_A}{\partial x} + v\frac{\partial C_A}{\partial y} + w\frac{\partial C_A}{\partial z}\right) + \frac{\partial C_A}{\partial t} = \frac{DC_A}{Dt}$$

$$\vec{\vartheta}.\vec{\nabla}C_A = \nabla N_A = \nabla\left(-D_{AB}\nabla C_A\right) =$$
$$= \frac{\partial^2 C_A}{\partial x^2} + \frac{\partial^2 C_A}{\partial y^2} + \frac{\partial^2 C_A}{\partial z^2} \qquad \text{eq.AN3 - 46}$$

Combining eq.AN3 - 44 , eq.AN3 - 45 and eq.AN3 - 46 eq.AN3 - 47

$$\left(u\frac{\partial C_A}{\partial x} + v\frac{\partial C_A}{\partial y} + w\frac{\partial C_A}{\partial z}\right) - D_{AB}.\left(\frac{\partial^2 C_A}{\partial x^2} + \frac{\partial^2 C_A}{\partial y^2} + \frac{\partial^2 C_A}{\partial z^2}\right) + \frac{\partial C_A}{\partial t} - R_A = 0$$

If there is no fluid motion, $\vec{\vartheta} = 0$; $R_A = 0$ or

$$\frac{\partial C_A}{\partial t} = D_{AB}.\left(\frac{\partial^2 C_A}{\partial x^2} + \frac{\partial^2 C_A}{\partial y^2} + \frac{\partial^2 C_A}{\partial z^2}\right) \qquad \text{eq.AN3 - 48}$$

Assumptions

Flow dimension: 2D (x-y) (length and width >>thickness); $\frac{\partial()}{\partial z} = 0$; $w = 0$;

Steady-State: $\frac{\partial(..)}{\partial t} = 0$

No chemical reaction : $R_A = 0$

Constant thermo physical properties: ρ, D_{AB}

Developed flow: (length>>thickness): $\frac{\partial(..)}{\partial x} = 0$ $\frac{\partial^2 C_A}{\partial x^2} << \frac{\partial^2 C_A}{\partial y^2}$

$$\left(u\frac{\partial C_A}{\partial x} + v\frac{\partial C_A}{\partial y}\right) = D_{AB}.\left(\frac{\partial^2 C_A}{\partial x^2}\right) \qquad \text{eq.AN3 - 49}$$

Newton's Law for the fluid (Mass Transfer by Convection)

$$N''_{A,S} = m.(C_{A,S} - C_{A,\infty})$$ eq.AN3 - 50

where m is the mass transfer coefficient by convection.

Combining eq.AN3 - 29 and eq.AN3 - 50

$$N''_{A,S} = -D_{AB}\left.\frac{\partial C_A}{\partial y}\right|_{y=0} = m.(C_{A,S} - C_{A,\infty})$$

$$m = \frac{-D_{AB}\left.\frac{\partial C_A}{\partial y}\right|_{y=0}}{(C_{A,S} - C_{A,\infty})} \equiv \frac{D_{AB}\big|_{y=\delta_C}}{\delta_C}$$ eq.AN3 - 51

where

$$\left.\frac{\partial C_A}{\partial y}\right|_{y=\delta_C} \equiv \frac{(C_{A,\infty} - C_{A,S})}{\delta_C} = \left.\frac{\partial C_A}{\partial y}\right|_{y=\delta_C}$$

Mass Continuity Equation

moving fluids, one dimension (y-direction), specie A

$$N_{Ay} = -D_{AB}\frac{\partial C_A}{\partial y} + X_A.(N_{Ay} + N_{By})$$ eq.AN3 - 52

For a gaseous media (ideal gas)

$$X_A = \frac{p_A}{P} = n_A.\frac{R.T}{V} = C_A.R.T \Rightarrow C_A = \frac{p_A}{R.T}$$ eq.AN3 - 53

$$C = \frac{n_A + n_B}{V} \therefore X_A = \frac{n_A}{n_A + n_B} \Rightarrow C_A = C.X_A$$

$$C = \frac{p_A}{R.T.X_A} = \frac{p_A}{R.T.\frac{p_A}{p}} = \frac{p}{R.T}$$

$$N_{Ay} = -CD_{AB}\frac{\partial X_A}{\partial y} + X_A.(N_{Ay} + N_{By}) = -\frac{p}{R.T}D_{AB}\frac{\partial X_A}{\partial y} + X_A.(N_{Ay} + N_{By})$$ eq.AN3 - 54

$$N_{Ay} = -CD_{AB}\frac{\partial\, p_A/p}{\partial y} + p_A/p.(N_{Ay} + N_{By}) = -\frac{1}{R.T}D_{AB}\frac{\partial p_A}{\partial y} + p_A/p.(N_{Ay} + N_{By})$$ eq.AN3 - 55

If p=1 atm

$$N_{Ay} = -\frac{1}{R.T}D_{AB}\frac{\partial p_A}{\partial y} + p_A.(N_{Ay} + N_{By})$$ eq.AN3 - 56

Hence, regarding the mechanisms of mass and heat transfer occurring simultaneously, and assuming:

$$\left.\frac{\partial C_A}{\partial y}\right|_{y=0} \approx \frac{\Delta C_A}{\Delta y} \text{ and } (C_{A,S} - C_{A,\infty}) \approx \Delta C_A$$

$$\left.\frac{\partial T}{\partial y}\right|_{y=0} \approx \frac{\Delta T}{\Delta y} \text{ and } (T_S - T_\infty) \approx \Delta T$$

Simplified relations should be stated, as presented below

$$m = \frac{D_{AB}}{\delta_C} \qquad \text{eq.AN3 - 57}$$

$$h = \frac{k_f}{\delta_T} \qquad \text{eq.AN3 - 58}$$

Boundary Layers and Generalized Equations

Convective Coefficients

Heat transfer through boundary layer obeys laws similar to those which apply to mass transfer through a concentration boundary layer as well the momentum transfer.

The boundary layer equations can be generalized applying independent and dimensionless variables. Examples:

Size eq.AN3 - 59

$$x^* \equiv \frac{x}{L};\ r^* \equiv \frac{r}{R}$$

Velocity eq.AN3 - 60

$$u^* \equiv \frac{u}{\vartheta}$$

Temperature eq.AN3 - 61

$$T^* \equiv \frac{T - T_S}{T_\infty - T_S}$$

Concentration eq.AN3 - 62

$$C_A^* \equiv \frac{C_A - C_{A,S}}{C_{A,\infty} - C_{A,S}}$$

Dimensionless parameters provide the comparison of results for momentum, heat and mass transfer estimates for similar geometries, but submitted to different convective conditions, such as: fluid properties, fluid velocity and surface dimension.

For the Velocity Boundary Layer

$$\left[v\frac{du^*}{dy^*} \right] = \frac{\mu}{\rho}\left(\frac{\partial^2 u^*}{\partial y^{*2}} \right) = \frac{1}{\mathrm{Re}_L}\left(\frac{\partial^2 u^*}{\partial y^{*2}} \right) \qquad \text{eq.AN3 - 63}$$

The Re Reynolds number means the ratio of two types of force acting on the fluid:

(inertial forces) $F_I \approx \frac{\vartheta^2}{L}$ /(viscous forces) $F_V \approx \frac{\mu\vartheta}{L^2}$

(convective forces)/(viscous forces)

(fluid motion forces)/(momentum transport)

$$\mathrm{Re} = \frac{\frac{\vartheta^2}{L}}{\frac{\mu\vartheta}{L^2}} = \frac{\rho.\vartheta.L}{\mu} = \frac{\vartheta.L}{\nu} \qquad \text{eq.AN3 - 64}$$

where μ is the viscosity, ν the kinematic viscosity and L the characteristic length of the solid submitted to the surrounding fluid.

For the Temperature Boundary Layer

$$u\frac{\partial T^*}{\partial x^*} + v\frac{\partial T^*}{\partial y^*} = \alpha\frac{\partial^2 T^*}{\partial y^{*2}} \equiv \frac{1}{\mathrm{Re}_L\,.\,\mathrm{Pr}}\frac{\partial^2 T^*}{\partial y^{*2}} \qquad \text{eq.AN3 - 65}$$

The Prandtl number relates to the ratio of viscosity and thermal diffusivity.

$$\mathrm{Pr} = \frac{\nu}{\alpha} = \frac{\mu/\rho}{k/\rho c_p} = \frac{\mu}{k}c_p \qquad \text{eq.AN3 - 66}$$

For the Concentration Boundary Layer

$$\left(u\frac{\partial C_A}{\partial x} + v\frac{\partial C_A}{\partial y} \right) = D_{AB}.\left(\frac{\partial^2 C_A}{\partial x^2} \right) \equiv \frac{1}{\mathrm{Re}_L\,.Sc}\left(\frac{\partial^2 C_A^*}{\partial x^{*2}} \right) \qquad \text{eq.AN3 - 67}$$

The Schmidt number Sc is the ratio of momentum diffusivity (kinematic viscosity) by the mass diffusivity

$$Sc = \frac{\nu}{D_{AB}} \qquad \text{eq.AN3 - 68}$$

The Nusselt number Nu is the ratio of resistances to heat transfer: the resistance in the boundary layer $1/h.A$ by the conduction resistance L/k_L. Measure the relative importance of the contributions of the convection and conduction mechanisms between a solid surface and a fluid. Furthermore, it can be stated that Nu is equal to the dimensionless temperature gradient, supporting the estimate the heat transfer by convection.

$$Nu = \frac{q'_{convection}}{q'_{conduction}} = \frac{h.(V_S/A_S)}{k_L} = f(x^*, \mathrm{Re}_L, \mathrm{Pr}) \qquad \text{eq.AN3 - 69}$$

$$h = \frac{-k_f . \frac{\partial T}{\partial y}}{(T_S - T_\infty)} = \frac{-k_f (T_\infty - T_S)}{(T_S - T_\infty)} \frac{\partial T^*}{\partial y^*}$$

$$\frac{\partial T^*}{\partial y^*} \equiv \frac{h(V_S/A_S)}{k_L} \equiv Nu$$

V_S/A_S is known as the characteristic dimension of the solid.

The difference between the Nusselt number and the Biot number lies in the fact that the heat transfer coefficient h in the case of relates to the heat conductivity of the medium (liquid phase) in which the heat transfer takes place as the immediate heat source.

The Sherwood number is the ratio of the mass convective coefficient by the mass diffusivity coefficient. Also, it can be said that is equal to the dimensionless concentration gradient.

$$Sh = \frac{m.(V_S/A_S)}{D_{AB}} = f(x^*, \mathrm{Re}_L, Sc) \qquad \text{eq.AN3 - 70}$$

$$m = \frac{-D_{AB} \frac{\partial C_A}{\partial y}}{(C_{A,S} - C_{A,\infty})} \equiv \frac{-D_{AB}(C_{A,\infty} - C_{A,S})}{(C_{A,S} - C_{A,\infty})} \frac{\partial C^*_A}{\partial y^*}$$

$$\frac{\partial C^*_A}{\partial y^*} \equiv \frac{m.(V_S/A_S)}{D_{AB}}$$

The Biot number Bi is the ratio of resistances to heat transfer: the resistance in the boundary layer h by the conduction resistance in the solid k_S

$$Bi = \frac{h.(V_S / A_S)}{k_S} \qquad \text{eq.AN3 - 71}$$